Draft version November 21, 2023
Typeset using LaTeX **twocolumn** style in AASTeX631

Identification of Intermediate-mass Black Hole Candidates Among a Sample of Sd Galaxies

Benjamin L. Davis [1,2] Alister W. Graham [1] Roberto Soria [3,4,5] Zehao Jin (金泽灏) [2]
Igor D. Karachentsev [6] Valentina E. Karachentseva,[7] and Elena D'Onghia [8]

[1] *Centre for Astrophysics and Supercomputing, Swinburne University of Technology, Hawthorn, VIC 3122, Australia*
[2] *Center for Astrophysics and Space Science (CASS), New York University Abu Dhabi, PO Box 129188, Abu Dhabi, UAE*
[3] *College of Astronomy and Space Sciences, University of the Chinese Academy of Sciences, Beijing 100049, China*
[4] *International Centre for Radio Astronomy Research, Curtin University, GPO Box U1987, Perth, WA 6845, Australia*
[5] *Sydney Institute for Astronomy, School of Physics A28, The University of Sydney, Sydney, NSW 2006, Australia*
[6] *Special Astrophysical Observatory, Russian Academy of Sciences, NÁrkhyz 369167, Russia*
[7] *Main Astronomical Observatory of National Academy of Sciences of Ukraine, Kyiv 03143, Ukraine*
[8] *Astronomy Department, University of Wisconsin, Madison, WI 53706, USA*

(Received November 21, 2023)

Submitted to *The Astrophysical Journal*

ABSTRACT

We have analyzed images of every northern hemisphere Sd galaxy listed in the Third Reference Catalogue of Bright Galaxies (RC3) with a relatively face-on inclination ($\theta \leq 30°$). Specifically, we have measured the spiral arms' winding angle, ϕ, in 85 galaxies. We have applied a novel black hole mass planar scaling relation involving the rotational velocities (from the literature) and pitch angles of each galaxy to predict central black hole masses. This yielded 23 galaxies, each having at least a 50% chance of hosting a central intermediate-mass black hole (IMBH), $10^2 < M_\bullet \leq 10^5\,\mathrm{M}_\odot$. These 23 nearby ($\lesssim$50 Mpc) targets may be suitable for an array of follow-up observations to check for active nuclei. Based on our full sample of 85 Sd galaxies, we estimate that the typical Sd galaxy (which tends to be bulgeless) harbors a black hole with $\log(M_\bullet/\mathrm{M}_\odot) = 6.00\pm0.14$, but with a 27.7% chance of hosting an IMBH, making this morphological type of galaxy fertile ground for hunting elusive IMBHs. Thus, we find that a $\sim 10^6\,\mathrm{M}_\odot$ black hole corresponds roughly to the onset of bulge development and serves as a conspicuous waypoint along the galaxy–SMBH coevolution journey. Our survey suggests that >1.22% of bright galaxies ($B_\mathrm{T} \lesssim 15.5$ mag) in the local Universe host an IMBH (*i.e.*, the "occupation fraction"), which implies a number density $>4.96\times10^{-6}\,\mathrm{Mpc}^{-3}$ for central IMBHs. Finally, we observe that Sd galaxies exhibit an unexpected diversity of properties that resemble the general population of spiral galaxies, albeit with an enhanced signature of the eponymous prototypical traits (*i.e.*, low masses, loosely wound spiral arms, and smaller rotational velocities).

Keywords: Astrostatistics (1882) — Galaxy evolution (594) — Hubble classification scheme (757) — Intermediate-mass black holes (816) — Late-type galaxies (907) — Regression (1914) — Scaling relations (2031) — Spiral galaxies (1560) — Spiral pitch angle (1561)

1. INTRODUCTION

Intermediate-mass black holes (IMBHs) could be characterized as the rare larval form of black holes. Announced within a span of just three years, astronomers built upon a century of black hole research[1] to obtain emphatic evidence for the embryonic and adult forms of black holes: stellar-mass (Abbott et al. 2016) and

Corresponding author: Benjamin L. Davis
ben.davis@nyu.edu

[1] See Graham (2016a) for key results and a detailed timeline of black hole research.

supermassive (Event Horizon Telescope Collaboration et al. 2019, 2022) black holes (SMBHs), respectively. However, speculation abounds concerning the intervening IMBH category that bridges the mass gap between stellar-mass and SMBHs. The gap in our knowledge is akin to a boxing league that has lightweight and heavyweight divisions, but no middleweight division. In which, there are three possibilities: (i) individual boxers have always been either lightweight or heavyweight, (ii) middleweight boxers always gain weight rapidly to become heavyweights, or (iii) there is an underground fighting league for middleweights that we are not privy to. Thus, we are on a quest to find evidence of scenario (iii) by tracking down clandestine IMBHs in their galactic lairs.

Perhaps the first evidence of the missing demographical category of black holes came at the turn of the millennium with the identification of an IMBH with a mass $>700\,M_\odot$ in M82 (Matsushita et al. 2000; Kaaret et al. 2001; Ebisuzaki et al. 2001; Matsumoto et al. 2001). Still, almost a quarter-century later, obtaining direct confirmation of IMBHs is not easy (see Mezcua 2017; Koliopanos 2017; Greene et al. 2020, for recent reviews). Even if one could prognosticate with certainty where to look for an IMBH, the telescope resources and time investment to garner definitive proof of IMBHs is significant (see Graham et al. 2021b, their §5). It is for these reasons that reconnaissance work is required to preselect the galaxies that are likely to harbor IMBHs. Such scouting studies will become invaluable to the world's best observatories as they look for IMBHs.

Large surveys will surely play a pivotal role in the search for IMBHs. Data mining of preexisting surveys can be a promising avenue for selection of candidates. Furthermore, large survey telescopes like the Vera C. Rubin Observatory (née Large Synoptic Survey Telescope; Tyson 2002) and the Einstein Probe (Yuan et al. 2022) are expected to find vast numbers of active galactic nuclei (AGNs), tidal disruption events (TDEs), and likely IMBHs. Careful filtering will be required to sort through the immense quantity of data produced to efficiently identify IMBH candidates.

One of the best methods for predicting black hole masses in galaxies is via black hole mass scaling relations (*e.g.*, Bennert et al. 2011; Graham et al. 2015; Graham 2016a; D'Onofrio et al. 2021; Izquierdo-Villalba et al. 2023). By identifying galaxies that reside at the same extreme end of multiple scaling relations, the success of their combined predictive power becomes more probable (Koliopanos et al. 2017; Graham & Soria 2019; Graham et al. 2019, 2021a,b; Davis & Graham 2021). Furthermore, because extrapolating is inherently uncertain, it is safer to extrapolate from multiple relations and look for agreement rather than trusting that a single relation holds beyond its defined range. Therefore, we seek a class of galaxy that consistently occupies the extremities of separate black hole mass scaling relations. Moreover, we effectively entwine the separate scaling relations by applying a novel trivariate relationship (Davis & Jin 2023).

Late-type spiral (*e.g.*, Sd) galaxies are the most compatible morphological class of galaxy for the focus of our experiment. Sd galaxies tick all the boxes in a census of galaxies that place them in a rare demographic category which is highly likely to cohabit with IMBHs.[2] Sd galaxies have open spiral structures, low total masses, small central velocity dispersions, slow rotational velocities, and are likely bulgeless; all such traits establish environments that should be ripe for the existence of IMBHs. Moreover, their structure is regular enough to not place them in peculiar or Magellanic type distinctions. The preponderance of low-mass, disk-dominated, bulgeless galaxies in our sample also distinguish our galaxies as having lived relatively merger-free lives. This creates an ideal scenario to conduct a clean test of IMBH growth in the absence of external influences on nuclear black holes that must have evolved in relative isolation (unlike Sm galaxies). Indeed, it is expected that the galaxy merger fraction monotonically increases as a function of stellar mass (Guzmán-Ortega et al. 2023) and bulge mass (Graham 2023a). Nonetheless, evidence shows that non-merger processes alone are sufficient to fuel massive black hole growth in galaxies (Smethurst et al. 2021) and sustain coevolution between SMBHs and their host galaxies (Smethurst et al. 2023).

The ongoing pursuit of IMBHs has seen significant recent contributions. Using the *Chandra* X-ray Observatory (CXO; Weisskopf et al. 2000), the "Chandra Virgo Cluster Survey of Spiral Galaxies" (Soria et al. 2022, see also Chilingarian et al. 2018 and Bi et al. 2020) obtained long exposures for spiral galaxies in the Virgo Cluster.

[2] We note that dwarf early-type galaxies (particularly low-mass S0 galaxies) are also good candidates to host IMBHs (Graham & Soria 2019). Furthermore, they have been shown to occasionally possess faint disk substructure, including bars and spiral arms, the latter of which can be quantified via pitch angle measurements (Jerjen et al. 2000; Lisker et al. 2006; Michea et al. 2021). However, the oft-hidden volute structure (*if* it exists) requires significant image processing to extract the embedded disk component, which itself has been historically missed even in bright early-type galaxies. Specifically, Lisker et al. (2006) found that 41 out of the 476 (8.6%) dwarf early-type galaxies in their sample showed "possible, probable, or unambiguous disk features." Although, the semblance of spiral structure in dwarf early-type galaxies could be caused by tidal triggering resulting from the cluster harassment of passive dwarf galaxies (Smith et al. 2021b).

When combined with archival data, this project has X-ray imaging for all spiral galaxies in the Virgo Cluster with star-formation rates $\gtrsim 1\,\mathrm{M}_\odot\,\mathrm{yr}^{-1}$. Early identification of nuclear X-ray point sources from the archival CXO data, coupled with black hole mass scaling relations, yielded $3 + 11$ strong[3] IMBH candidates (Graham et al. 2019, 2021b). Karachentsev & Karachentseva (2019) collated a catalog of 220 face-on bulgeless galaxies, approximately half of which exhibit unresolved nuclei. Because nuclear star clusters (NSCs) are known to scale with their host galaxies (Balcells et al. 2003; Graham 2003; Wehner & Harris 2006; den Brok et al. 2014; Georgiev et al. 2016; Sánchez-Janssen et al. 2019; Pechetti et al. 2020) and their central black holes (Graham & Spitler 2009; Scott & Graham 2013; Georgiev et al. 2016; Graham 2016b, 2020; Neumayer et al. 2020), such a catalog is a valuable reference of potential IMBH host galaxies.

Sd galaxies are certainly not the only place where IMBHs might exist. McKernan et al. (2012) envision an efficient process by which IMBHs may be efficiently grown in AGNs in the disks surrounding SMBHs. There might be IMBHs roaming our Galaxy (Schödel et al. 2005; Oka et al. 2017; Tsuboi et al. 2017, 2019, 2020; Takekawa et al. 2019, 2020; Zhu et al. 2020; Reid & Brunthaler 2020; Gravity Collaboration et al. 2020; Weller et al. 2022) or in its satellites that reveal themselves more readily than IMBHs in extragalactic environments.[4] Indeed, Nguyen et al. (2019) estimated a black hole mass ($M_\bullet \equiv M_{\rm BH}$) of $\log(M_\bullet/\mathrm{M}_\odot) = 3.83^{+0.43}_{-0.60}$ in Messier 110 (a dwarf elliptical satellite of the Andromeda Galaxy) via stellar dynamical modeling. Verily, not all fish are in the oceans but also rivers, ponds, and lakes. Analogously, Sd galaxies represent the major fishing areas for catching potential IMBHs. It is our endeavor here to establish: in general, (i) how common IMBHs might be in Sd galaxies and explicitly, (ii) which Sd galaxies pose the most promising potential for future studies to search for IMBHs.

We define our sample of Sd galaxies in §2, and apply a planar black hole mass scaling relation to the collection of galaxies (in §3). In §4, we present the results and statistics for our sample and identify our targets of interest. Additionally, we discuss other observational considerations such as AGNs and X-ray point sources. Finally, we provide a discussion (in §5) on our findings for Sd galaxies, detail the implications from IMBH research, consider the prospects of detecting IMBHs in our sample, and consider the outlook for follow-up investigations. We represent masses (M) throughout this work as logarithmic (solar) masses ($\mathcal{M}$), such that $\mathcal{M} \equiv \log(M/\mathrm{M}_\odot)$. Stellar masses have all been adjusted to conform with the Chabrier (2003) initial mass function[5] and we assume cosmographic parameters from Planck Collaboration et al. (2020). All uncertainties are quoted at $1\,\sigma \equiv 68.3\%$ confidence intervals; median absolute deviations are given as uncertainties associated with medians.

2. SAMPLE OF GALAXIES

We assembled a sample of Sd (*i.e.*, SAd, SABd, and SBd) type galaxies (Shapley & Paraskevopoulos 1940; de Vaucouleurs 1959; Graham 2019). We focussed on the Sd, rather than Sc and earlier types, because of the expected larger spiral-arm winding angles; open spiral arms correlate with low black hole masses (Seigar et al. 2008; Berrier et al. 2013; Davis et al. 2017). The Magellanic-like Sm, and Sdm, (nor irregular) galaxies were not included because of their inherent disrupted and asymmetric structures.[6] Sd galaxies exhibit open spiral-arm structures and possess very faint (or no) bulges; they are ideal galaxies to host IMBHs. Because the bulge-to-total flux ratio (B/T) of Sd galaxies are low enough[7] to be considered "bulgeless,"[8] traditional (black hole mass)–(bulge mass) and (black hole mass)–(Sérsic index) relations are problematic, indicating a population of galaxies that likely possess small (or no) nuclear black holes.[9]

Bulgeless galaxies may still be analyzed with other black hole mass scaling relations that are not dependent on bulge masses, but some other physical property, such as spiral-arm pitch angle (Seigar et al. 2008; Berrier et al. 2013; Davis 2015; Davis et al. 2017), central velocity dispersion (Ferrarese & Merritt 2000; Gebhardt et al. 2000; Sahu et al. 2019a), total stellar mass (Beifiori et al. 2012; Davis et al. 2018; Sahu et al. 2019b; Graham

[3] Here, *strong* candidates are those with both a predicted black hole mass $\lesssim 10^5\,\mathrm{M}_\odot$ and a centrally-located X-ray point source.

[4] Specifically, Paynter et al. (2021) estimated there are $\approx 4.6 \times 10^4$ IMBHs with masses between $\approx 10^4$–$10^5\,\mathrm{M}_\odot$ in the neighborhood of the Milky Way.

[5] See Davis et al. (2018, 2019b) for further details on how we homogenize stellar masses from various studies.

[6] Nevertheless, there is evidence that IMBHs may reside in irregular and/or Magellanic-type morphologies (*e.g.*, NGC 5408; Strohmayer & Mushotzky 2009).

[7] Observed in the B-band, the bulge-to-total flux ratio for Sd galaxies has been reported as 0.029 (Simien & de Vaucouleurs 1986) and $0.027^{+0.066}_{-0.016}$ (Graham & Worley 2008).

[8] For Sd galaxies, which typically lack conventional bulges, the central component proxy is likely a weak pseudobulge or "barge" (portmanteau of "bar" and "bulge").

[9] See Bohn et al. (2020) for a thorough list and discussion of known bulgeless galaxies with black hole mass estimates.

2023a),[10] and rotational velocity (Ferrarese 2002; Sabra et al. 2015; Davis et al. 2019c; Smith et al. 2021a).[11] The measurement of spiral-arm pitch angle (ϕ) requires a spiral galaxy first to be corrected to a face-on orientation via a deprojection of its apparent inclination with respect to the plane of the sky (see Davis et al. 2012, figure 2). Because of this necessity, face-on galaxies are far easier to measure, with pitch angles becoming progressively harder to measure for more inclined galaxies and impossible for edge-on galaxies. For this reason, we have selected our sample of spiral galaxies to be close to face-on. Additionally, dust/inclination effects are minimized for galaxies when they are near to face-on.

We have constructed this study to take advantage of the remarkably low level of scatter for black hole mass estimates from the $M_\bullet$–ϕ relation. The usual go-to black hole mass scaling relation for the majority of studies has been the $M_\bullet$–σ_0 relation, due to its low level of scatter and availability of central velocity dispersion (σ_0) measurements. Indeed, central velocity dispersion is often described as the most fundamental black hole mass scaling relation parameter (*e.g.*, de Nicola et al. 2019). However, this is predominantly the case for early-type galaxies; for late-type galaxies, the scatter is higher and σ_0 measurements are less common. From a common sample of 44 spiral galaxies, Davis et al. (2017) showed that the intrinsic scatter for the $M_\bullet$–σ_0 relation is 0.21 dex higher than that of the $M_\bullet$–ϕ relation.

For the selection of our galaxies, we turned to the Third Reference Catalogue of Bright Galaxies (de Vaucouleurs et al. 1991, hereafter RC3). The full RC3 sample contains 23,022 galaxies (17,801 with morphological classifications) with apparent diameters larger than one arcminute ($D_{25} > 1'$), total B-band magnitudes brighter than about 15.5 mag (Vega $B_{\rm T} \lesssim 15.5$ mag), and recessional velocities $cz < 15{,}000\,{\rm km\,s^{-1}}$ ($z < 0.050$; luminosity distances out to $d = 230$ Mpc). Using their online database,[12] we selected a sample consisting of all Sd galaxies (Hubble sequence morphological stage, $T = 7.0$)[13] with inclination angles (θ) such that $0° \leq \theta \leq 30°$,[14] and in the northern celestial hemisphere (declinations greater than 0°). These selection criteria yielded a sample of 85 spiral galaxies (see Table 1). We chose to restrict our sample to the northern sky so that our entire sample would be visible by extensive sky surveys such as Pan-STARRS1 and SDSS to assure uniform access to high-quality imaging of volute structure to facilitate the measurement of spiral-arm pitch angles. Therefore, our sample should represent roughly 1/15 of the entire RC3 sample of Sd galaxies (*i.e.*, half of the sky and $1 - \cos 30°$ of all random inclination orientations). In actuality, there are 787 Sd galaxies in the RC3, thus we have selected $85/787 \approx 11\%$, *cf.* $1/15 \approx 6.7\%$.

[10] Moreover, the fact that black holes follow the (black hole mass)–(host stellar mass) relation even in bulgeless galaxies indicates that massive black holes may form before stellar bulges in galaxies (*e.g.*, Chen et al. 2023d).

[11] The total number of globular clusters bound to a galaxy is also an intriguing proxy for its central black hole mass (Burkert & Tremaine 2010; Harris & Harris 2011; Harris et al. 2014; González-Lópezlira et al. 2022). Notably, Bluck et al. (2023) find that the stellar gravitational potential of a galaxy is strongly correlated with SMBH mass, which is easy to measure in both observational and simulated data.

[12] https://heasarc.gsfc.nasa.gov/W3Browse/all/rc3.html

[13] In their study of spiral galaxies in the RC3, Ma et al. (1999) indeed found that Sd types had the highest observed pitch angles, $|\bar{\phi}| = 25.^\circ00$.

[14] Here, the inclination angle is determined from the mean ratio ($\log {\rm R}_{25}$) of the major isophotal diameter ($\rm D_{25}$) to the minor isophotal diameter ($\rm d_{25}$) measured at or reduced to the B-band surface brightness level $\mu_B = 25.0\,{\rm mag\,arcsec^{-2}}$. Therefore, we selected $0 \leq \log {\rm R}_{25} \lesssim 0.06$ because $\theta \equiv \sec^{-1}({\rm R}_{25})$.

Table 1. Sample of 85 Sd Galaxies

Galaxy	Distance	BPT	CXO Exp	CXO #	$\lvert\phi\rvert$	σ_0	$\mathcal{M}_{\rm gal,\star}$	θ	$v_{\rm max}$	$\mathcal{M}_\bullet$	$P(\mathcal{M}_\bullet \le 5)$	$n\,\sigma$
	[Mpc]		[ks]		[°]	$\left[\frac{\rm km}{\rm s}\right]$	[dex]	[°]	$\left[\frac{\rm km}{\rm s}\right]$	[dex]	[%]	[σ]
(1)	(2)	(3)	(4)	(5)	(6)	(7)	(8)	(9)	(10)	(11)	(12)	(13)
IC 951	62.2 ± 7.2	H II	···	···	9.5 ± 2.9	···	10.2 ± 0.2	17 ± 2	199 ± 29	7.6 ± 0.4	≈0.0	−5.9
IC 1221	74.9 ± 6.5	H II	5	0	22.7 ± 3.9	···	10.3 ± 0.1	18 ± 1	62 ± 5	4.2 ± 0.5	93.3	1.5
IC 1774	41.8 ± 5.8	···	···	···	22.8 ± 2.4	···	9.9 ± 0.2	43 ± 2	99 ± 5	5.0 ± 0.4	49.7	0.0
IC 1776	40.9 ± 6.1	···	···	···	17.9 ± 3.0	···	9.9 ± 0.2	28 ± 1	99 ± 3	5.6 ± 0.4	8.0	−1.4
NGC 2500	12.0 ± 9.4	···	3	7	16.3 ± 1.3	···	9.6 ± 0.7	28 ± 11	90 ± 34	5.6 ± 0.7	20.7	−0.8
NGC 2657	59.0 ± 7.2	···	···	···	15.8 ± 4.5	···	10.4 ± 0.2	35 ± 3	144 ± 11	6.4 ± 0.5	0.4	−2.6
NGC 3906	19.0 ± 8.0	···	5	0	16.6 ± 1.9	···	9.6 ± 0.4	42 ± 4	134 ± 12	6.2 ± 0.3	≈0.0	−3.6
NGC 3913	17.9 ± 7.5	···	5	0	12.9 ± 0.2	···	9.5 ± 0.4	16 ± 4	69 ± 19	5.5 ± 0.5	19.0	−0.9
NGC 4393	7.7 ± 1.3	···	5	0	9.7 ± 2.8	···	8.6 ± 0.2	56 ± 1	62 ± 2	5.6 ± 0.4	4.7	−1.7
NGC 5148	87.8 ± 6.5	···	7	0	18.7 ± 3.7	···	10.1 ± 0.1	25 ± 1	84 ± 6	5.2 ± 0.5	34.5	−0.4
NGC 5668	21.3 ± 6.2	···	···	···	27.3 ± 2.8	53 ± 8	10.1 ± 0.3	15 ± 1	152 ± 8	5.2 ± 0.4	31.2	−0.5
NGC 6617	91.4 ± 6.5	···	···	···	13.3 ± 1.9	···	10.2 ± 0.2	52 ± 1	144 ± 6	6.7 ± 0.3	≈0.0	−5.5
NGC 6687	44.3 ± 6.0	···	···	···	24.5 ± 0.6	···	9.8 ± 0.2	42 ± 0	101 ± 19 †	4.9 ± 0.4	63.5	0.3
NGC 7363	91.2 ± 6.6	···	···	···	10.8 ± 1.3	···	10.5 ± 0.2	29 ± 1	242 ± 14	7.8 ± 0.3	≈0.0	−10.1
NGC 7437	26.0 ± 5.9	···	···	···	18.0 ± 1.4	···	9.6 ± 0.3	17 ± 1	153 ± 13	6.3 ± 0.3	≈0.0	−4.2
NGC 7535	58.5 ± 6.2	···	···	···	13.2 ± 1.0	···	10.2 ± 0.1	28 ± 2	109 ± 8	6.2 ± 0.3	≈0.0	−4.3
UGC 42	69.2 ± 6.3	···	···	···	16.0 ± 4.8	···	9.5 ± 0.2	41 ± 6	95 ± 11	5.7 ± 0.6	12.2	−1.2
UGC 283	47.5 ± 6.0	···	···	···	12.6 ± 4.0	···	9.8 ± 0.2	45 ± 1	144 ± 9	6.8 ± 0.5	≈0.0	−3.6
UGC 336	75.0 ± 6.5	···	···	···	16.4 ± 3.1	···	10.0 ± 0.2	35 ± 3	180 ± 16	6.7 ± 0.4	≈0.0	−4.1
UGC 384	50.9 ± 5.3	···	···	···	19.0 ± 0.7	···	10.0 ± 0.2	45 ± 2	121 ± 6	5.8 ± 0.3	0.1	−3.1
UGC 1341	142.2 ± 6.6	···	···	···	10.8 ± 2.8	···	10.5 ± 0.1	32 ± 3	208 ± 18	7.6 ± 0.4	≈0.0	−6.6
UGC 1544	55.5 ± 5.4	···	···	···	33.1 ± 1.9	···	9.6 ± 0.2	53 ± 7	49 ± 5	2.5 ± 0.4	≈100.0	6.3
UGC 1606	104.9 ± 6.6	···	···	···	11.4 ± 4.7	···	9.9 ± 0.2	39 ± 2	152 ± 8	7.0 ± 0.5	≈0.0	−3.7
UGC 1702	163.5 ± 6.6	···	···	···	5.8 ± 2.8	···	10.6 ± 0.2	20 ± 1	284 ± 14	8.6 ± 0.4	≈0.0	−9.8
UGC 1795	187.1 ± 6.6	···	···	···	23.3 ± 3.6	···	10.6 ± 0.2	59 ± 3	226 ± 18	6.4 ± 0.5	0.3	−2.8
UGC 1833	52.1 ± 5.4	···	···	···	25.3 ± 2.1	···	9.9 ± 0.2	61 ± 3	82 ± 4	4.4 ± 0.3	95.6	1.7
UGC 1897	109.0 ± 6.6	···	···	···	28.7 ± 4.9	···	10.2 ± 0.2	40 ± 1	132 ± 6	4.8 ± 0.7	61.8	0.3
UGC 2008	55.8 ± 5.5	···	···	···	21.6 ± 3.5	···	9.4 ± 0.2	28 ± 3	109 ± 12	5.3 ± 0.5	26.3	−0.6
UGC 2109	39.6 ± 5.3	···	···	···	17.0 ± 2.0	···	10.0 ± 0.2	39 ± 2	112 ± 5	5.9 ± 0.3	0.4	−2.7
UGC 2437	40.1 ± 5.9	···	···	···	31.8 ± 3.7	···	10.0 ± 0.2	39 ± 2	131 ± 9	4.4 ± 0.6	86.4	1.1
UGC 2458	218.3 ± 6.6	···	···	···	11.9 ± 0.9	···	10.7 ± 0.2	36 ± 2	175 ± 34 †	7.2 ± 0.4	≈0.0	−5.2
UGC 2623	47.5 ± 5.3	···	···	···	11.6 ± 3.0	···	9.8 ± 0.2	35 ± 4	81 ± 9	5.9 ± 0.4	2.1	−2.0
UGC 2671	90.6 ± 6.4	···	···	···	16.6 ± 1.7	···	10.1 ± 0.2	25 ± 4	187 ± 31	6.8 ± 0.4	≈0.0	−4.4
UGC 2935	56.8 ± 6.2	···	···	···	24.1 ± 2.9	···	9.1 ± 0.2	62 ± 2	33 ± 2	3.0 ± 0.4	≈100.0	4.9
UGC 3074	52.7 ± 6.1	···	···	···	17.3 ± 0.2	···	9.9 ± 0.2	23 ± 4	121 ± 22	6.0 ± 0.4	0.6	−2.5
UGC 3364	59.2 ± 6.4	···	···	···	16.5 ± 2.7	···	9.7 ± 0.2	33 ± 3	109 ± 9	5.9 ± 0.4	1.3	−2.2
UGC 3402	222.9 ± 6.6	···	···	···	16.6 ± 1.3	···	10.9 ± 0.2	34 ± 1	202 ± 40 †	6.9 ± 0.4	≈0.0	−4.5
UGC 3702	65.8 ± 6.6	···	···	···	16.2 ± 2.8	···	10.0 ± 0.2	27 ± 1	65 ± 4	5.0 ± 0.4	48.0	0.0
UGC 3799	81.5 ± 6.7	···	···	···	10.7 ± 1.4	···	10.4 ± 0.2	39 ± 1	144 ± 5	6.9 ± 0.3	≈0.0	−7.0
UGC 3826	26.8 ± 7.0	···	···	···	19.9 ± 4.8	···	9.3 ± 0.3	40 ± 4	32 ± 3	3.4 ± 0.6	99.6	2.7
UGC 3875	71.6 ± 6.7	···	···	···	21.4 ± 3.8	···	10.0 ± 0.2	30 ± 5	171 ± 25	6.1 ± 0.5	2.0	−2.0
UGC 3949	89.9 ± 6.9	···	···	···	25.8 ± 0.3	70 ± 5 *	10.5 ± 0.1	32 ± 1	101 ± 6	4.7 ± 0.3	87.6	1.2
UGC 4077	62.0 ± 6.7	H II	···	···	31.1 ± 1.1	···	10.0 ± 0.2	33 ± 3	130 ± 12	4.5 ± 0.3	96.0	1.7
UGC 4363	48.8 ± 6.5	···	···	···	17.6 ± 4.2	···	9.8 ± 0.1	76 ± 1	36 ± 2	3.8 ± 0.5	98.7	2.2
UGC 4622	175.9 ± 6.8	Comp	···	···	23.4 ± 2.3	107 ± 8 *	10.9 ± 0.1	19 ± 1	201 ± 34 †	6.2 ± 0.5	0.6	−2.5
UGC 4831	62.2 ± 7.0	H II	···	···	15.9 ± 0.7	···	9.8 ± 0.2	26 ± 3	127 ± 16	6.2 ± 0.3	≈0.0	−3.7
UGC 5142	98.1 ± 7.3	···	···	···	9.9 ± 2.6	···	10.1 ± 0.2	36 ± 3	103 ± 8	6.5 ± 0.4	≈0.0	−3.9

Table 1 *continued*

Table 1 *(continued)*

			CXO									
Galaxy	Distance	BPT	Exp	#	$\lvert\phi\rvert$	σ_0	$\mathcal{M}_{\rm gal,\star}$	θ	$v_{\rm max}$	$\mathcal{M}_\bullet$	$P(\mathcal{M}_\bullet \leq 5)$	$n\,\sigma$
	[Mpc]		[ks]		[°]	$\left[\frac{\rm km}{\rm s}\right]$	[dex]	[°]	$\left[\frac{\rm km}{\rm s}\right]$	[dex]	[%]	[σ]
(1)	(2)	(3)	(4)	(5)	(6)	(7)	(8)	(9)	(10)	(11)	(12)	(13)
UGC 5344	62.0 ± 7.5	H II	···	···	15.3 ± 3.4	···	9.9 ± 0.2	28 ± 5	37 ± 6	4.1 ± 0.5	95.7	1.7
UGC 5460	20.6 ± 8.0	···	15	0	26.2 ± 2.2	···	9.4 ± 0.4	54 ± 4	46 ± 3	3.3 ± 0.4	≈100.0	4.6
UGC 6505	97.6 ± 6.8	···	···	···	10.0 ± 4.7	···	10.0 ± 0.2	19 ± 4	115 ± 21 †	6.6 ± 0.6	0.4	−2.7
UGC 6616	20.5 ± 7.4	···	···	···	28.6 ± 4.3	···	9.3 ± 0.4	30 ± 1	90 ± 5	4.2 ± 0.6	92.3	1.4
UGC 6893	84.2 ± 6.6	···	···	···	15.9 ± 4.1	···	10.0 ± 0.1	17 ± 8	187 ± 80	6.9 ± 0.9	1.7	−2.1
UGC 7942	7.0 ± 3.7	···	···	···	16.5 ± 1.3	···	8.1 ± 0.5	31 ± 14	35 ± 12 †	3.9 ± 0.6	95.7	1.7
UGC 8153	42.5 ± 7.2	H II	···	···	31.6 ± 3.5	···	9.8 ± 0.2	29 ± 3	111 ± 9	4.1 ± 0.5	94.4	1.6
UGC 8171	292.5 ± 7.4	AGN	···	···	22.7 ± 1.3	···	11.2 ± 0.1	25 ± 4	240 ± 40 †	6.6 ± 0.4	≈0.0	−3.9
UGC 8436	45.8 ± 7.3	H II	···	···	10.6 ± 1.2	···	9.6 ± 0.2	24 ± 8	71 ± 23	5.7 ± 0.6	11.4	−1.2
UGC 8611	41.4 ± 7.1	H II	···	···	16.4 ± 4.3	···	9.5 ± 0.2	43 ± 4	102 ± 8	5.8 ± 0.5	7.6	−1.4
UGC 8637	90.7 ± 6.4	H II	···	···	24.7 ± 3.3	···	10.3 ± 0.1	29 ± 7	97 ± 21	4.8 ± 0.6	65.5	0.4
UGC 8670	271.0 ± 7.4	···	···	···	20.9 ± 3.3	···	11.1 ± 0.1	18 ± 7	238 ± 39 †	6.7 ± 0.5	≈0.0	−3.4
UGC 9008	72.3 ± 6.6	H II	···	···	11.5 ± 4.6	···	9.9 ± 0.1	25 ± 5	130 ± 27	6.7 ± 0.6	0.4	−2.7
UGC 9010	98.6 ± 6.5	···	···	···	13.6 ± 0.9	···	10.1 ± 0.2	46 ± 3	150 ± 11	6.7 ± 0.3	≈0.0	−6.3
UGC 9042	108.9 ± 6.5	H II	···	···	11.0 ± 2.8	···	9.9 ± 0.2	20 ± 5	229 ± 59	7.7 ± 0.6	≈0.0	−4.7
UGC 9052	99.2 ± 6.8	···	···	···	15.4 ± 1.5	···	10.3 ± 0.2	28 ± 6	137 ± 24 †	6.4 ± 0.4	≈0.0	−3.4
UGC 9340	62.9 ± 6.6	H II	5	0	19.6 ± 2.4	···	9.9 ± 0.2	23 ± 10	144 ± 60	6.0 ± 0.8	9.9	−1.3
UGC 9722	95.9 ± 8.0	···	···	···	6.2 ± 4.7	···	10.0 ± 0.2	29 ± 6	113 ± 23 †	7.0 ± 0.6	0.1	−3.2
UGC 10020	31.5 ± 6.8	H II	···	···	19.2 ± 3.5	···	9.6 ± 0.2	19 ± 2	77 ± 7	5.0 ± 0.5	52.0	0.1
UGC 10146	102.2 ± 6.1	···	···	···	14.2 ± 2.9	···	10.1 ± 0.2	34 ± 1	127 ± 6	6.4 ± 0.4	≈0.0	−3.6
UGC 10440	59.1 ± 6.4	···	···	···	34.5 ± 1.9	···	9.6 ± 0.2	33 ± 7	68 ± 13	2.9 ± 0.5	≈100.0	4.4
UGC 10831	102.2 ± 6.1	···	···	···	20.2 ± 3.5	···	10.4 ± 0.1	41 ± 2	275 ± 18	7.1 ± 0.5	≈0.0	−4.5
UGC 10922	113.5 ± 6.4	···	···	···	16.8 ± 0.8	···	10.2 ± 0.2	25 ± 5	118 ± 24	6.0 ± 0.4	1.1	−2.3
UGC 11029	40.4 ± 5.9	···	···	···	24.3 ± 4.8	···	9.6 ± 0.2	39 ± 0	123 ± 5	5.2 ± 0.6	36.5	−0.3
UGC 11113	31.4 ± 6.1	···	···	···	19.7 ± 2.9	···	9.4 ± 0.2	54 ± 1	55 ± 2	4.3 ± 0.4	95.2	1.7
UGC 11386	102.5 ± 6.6	···	···	···	12.6 ± 2.7	···	10.2 ± 0.2	27 ± 3	146 ± 19	6.8 ± 0.4	≈0.0	−4.2
UGC 11515	41.3 ± 30.6	···	···	···	25.4 ± 0.3	···	10.1 ± 0.7	36 ± 2	109 ± 11	4.9 ± 0.3	66.6	0.4
UGC 11556	71.0 ± 6.2	···	···	···	23.8 ± 3.4	···	9.5 ± 0.2	30 ± 0	79 ± 3	4.5 ± 0.5	85.3	1.1
UGC 11653	47.6 ± 5.5	···	···	···	17.5 ± 2.2	···	9.7 ± 0.2	42 ± 3	108 ± 7	5.8 ± 0.3	1.5	−2.2
UGC 11699	58.4 ± 5.9	···	···	···	15.0 ± 1.3	···	9.8 ± 0.2	27 ± 4	103 ± 14	5.9 ± 0.4	0.4	−2.7
UGC 11728	108.1 ± 6.6	···	···	···	11.5 ± 3.2	···	10.4 ± 0.1	22 ± 3	103 ± 13	6.3 ± 0.5	0.2	−2.9
UGC 11992	42.8 ± 5.8	···	···	···	9.2 ± 2.0	···	9.4 ± 0.2	44 ± 2	103 ± 4	6.5 ± 0.3	≈0.0	−5.0
UGC 12008	104.9 ± 6.8	···	···	···	11.0 ± 4.5	···	10.3 ± 0.2	31 ± 3	210 ± 22	7.6 ± 0.5	≈0.0	−4.8
UGC 12015	100.4 ± 6.4	···	···	···	12.0 ± 4.7	···	10.2 ± 0.2	40 ± 2	99 ± 7	6.2 ± 0.5	1.4	−2.2
UGC 12176	123.5 ± 6.7	···	···	···	15.4 ± 3.9	···	10.5 ± 0.2	41 ± 3	52 ± 3	4.7 ± 0.5	73.1	0.6
UGC 12184	51.2 ± 6.1	···	···	···	16.0 ± 3.0	···	9.5 ± 0.1	19 ± 3	90 ± 14	5.6 ± 0.5	9.8	−1.3
UGC 12289	135.8 ± 6.6	···	···	···	24.0 ± 4.7	···	10.5 ± 0.2	29 ± 8	201 ± 53	6.1 ± 0.7	7.1	−1.5
UGC 12685	67.0 ± 6.3	···	···	···	20.7 ± 3.9	···	9.8 ± 0.2	28 ± 10	125 ± 40	5.7 ± 0.7	19.0	−0.9

Table 1 *continued*

Table 1 *(continued)*

			CXO									
Galaxy	Distance	BPT	Exp	#	$\lvert\phi\rvert$	σ_0	$\mathcal{M}_{\mathrm{gal},\star}$	θ	v_{max}	$\mathcal{M}_\bullet$	$P(\mathcal{M}_\bullet \leq 5)$	$n\,\sigma$
	[Mpc]		[ks]		[°]	$\left[\frac{\mathrm{km}}{\mathrm{s}}\right]$	[dex]	[°]	$\left[\frac{\mathrm{km}}{\mathrm{s}}\right]$	[dex]	[%]	[σ]
(1)	(2)	(3)	(4)	(5)	(6)	(7)	(8)	(9)	(10)	(11)	(12)	(13)

Note— **Column (1):** galaxy name. **Column (2):** luminosity distance (in Mpc) from HyperLeda (Makarov et al. 2014). Galaxies closer than 200 Mpc have been adjusted according to the Cosmicflows-3 Distance–Velocity Calculator (Kourkchi et al. 2020), available at the Extragalactic Distance Database (http://edd.ifa.hawaii.edu). Distances (d) less than 38 Mpc have computed expectation distances based on the smoothed velocity field from the Numerical Action Methods model of Shaya et al. (2017). 38 Mpc $< d <$ 200 Mpc have computed expectation distances based on the smoothed velocity field from the linear density field model of Graziani et al. (2019). Redshift-dependent distances are calibrated to the Planck Collaboration et al. (2020) cosmographic parameters. **Column (3):** the BPT [N II]/Hα versus [O III]/Hβ standard optical diagnostic classification. "H II" = H II-region-like galaxy, "AGN" = active galactic nucleus, and "Comp" = composite galaxy (likely to contain a metal-rich stellar population plus an AGN). **Column (4):** Chandra X-ray Observatory (CXO) exposure time (in ks) of the galaxy's nucleus. **Column (5):** the number of X-ray photons emanating from the galaxy's nucleus detected by the CXO. **Column (6):** absolute value of the *face-on* spiral-arm pitch angle (in degrees), derived primarily from Pan-STARRS1 imaging, and measured by the `2DFFT`, `SpArcFiRe`, and/or `Spirality` software packages. **Column (7):** central stellar velocity dispersion (in $\mathrm{km\,s^{-1}}$) from HyperLeda. **Column (8):** logarithm of the total galaxy stellar mass (in $\mathrm{M_\odot}$); we use the intrinsic K-band apparent magnitudes from HyperLeda, then converted to luminosity by correcting for distance, compensating for surface brightness dimming (Tolman 1930, 1934), and applying the solar absolute magnitude from Willmer (2018), which is multiplied by the mass-to-light ratio from Davis et al. (2019b, equation 8). **Column (9):** inclination angle (in degrees), determined via our pitch angle measurement process. **Column (10):** physical maximum velocity rotation (in $\mathrm{km\,s^{-1}}$) corrected for inclination, from HyperLeda. **Column (11):** predicted black hole mass from the planar relation of Davis & Jin (2023), *i.e.*, combining Columns (6) and (10). **Column (12):** probability that the central black hole is an IMBH, *i.e.*, $P(\mathcal{M}_\bullet \leq 5)$ (via Davis & Graham 2021, equation 7). **Column (13):** number of standard deviations below $10^5\,\mathrm{M_\odot}$, *i.e.*, $n\,\sigma = (5 - \mathcal{M}_\bullet)/\delta\mathcal{M}_\bullet$.

* Obtained from the NASA-Sloan Atlas (http://www.nsatlas.org). The 1.″5-radius-aperture-based σ_0 value was normalized to match the $0.595\,h^{-1}$ kpc-radius-aperture used in the homogenized system of HyperLeda via the prescriptions of Jorgensen et al. (1995).

† Velocity is estimated via the Tully-Fisher relation (Tully & Fisher 1977) as refined by Tiley et al. (2019).

3. PREDICTING BLACK HOLE MASSES

3.1. *The $M_\bullet$–ϕ Relation*

The $M_\bullet$–ϕ relation is the most natural black hole mass scaling relation for application to spiral galaxies. Furthermore, it exhibits the lowest level of intrinsic scatter ($\epsilon = 0.33 \pm 0.08$ dex from Davis et al. 2017) of any single black hole mass scaling relation for spiral galaxies. The logarithmic spiral pitch angle is the most-widely adopted metric for quantifying the geometric shape of spiral arms in disk galaxies. The $M_\bullet$–ϕ relation (Seigar et al. 2008; Berrier et al. 2013; Davis et al. 2017) can be used to predict central black holes in spiral galaxies and identify IMBH candidates (Graham et al. 2019; Treuthardt et al. 2019). The $M_\bullet$–ϕ relation is uniquely applicable to only spiral galaxies. Whereas most other black hole mass scaling relations may be employed for any morphological type of galaxy, such scaling relations are usually less accurate when derived from spiral galaxies alone. For example, Sahu et al. (2019a) found that the $M_\bullet$–σ_0 relation for late-type galaxies exhibits an intrinsic scatter that is 0.25 dex higher than the $M_\bullet$–σ_0 relation for early-type galaxies.

We have measured ϕ for all 85 galaxies in our sample (Column 6 of Table 1). We obtained g, r, i, z, and y images from Pan-STARRS1[15] (Chambers et al. 2016), and the image that best highlighted the spiral structure was adopted for the pitch angle measurement. Sloan Digital Sky Survey (SDSS) or Galaxy Evolution Explorer (GALEX) images were also consulted and used if the volute structure was better resolved. Galaxy images were first deprojected to a face-on orientation and then analyzed by a combination of software packages, including `2DFFT` (Davis et al. 2012, 2016), `SpArcFiRe` (Davis & Hayes 2014), and/or `Spirality` (Shields et al. 2015, 2022).[16]

3.2. *The $M_\bullet$–v_{max} Relation*

For most of our sample (75/85), we were able to obtain the physical maximum rotational velocities ($v_{\mathrm{max}} \equiv v_{\mathrm{rot}}$) from HyperLeda (Makarov et al. 2014). As for the remaining ten galaxies (see Table 1, Column 10), we estimated the rotational velocities by applying the Tully-Fisher relation (Tully & Fisher 1977) as refined by Tiley et al. (2019). The HyperLeda velocities are derived from the original line-of-sight velocities (from both 21-cm line widths and/or rotation curves) and subsequently corrected for inclination. Although we used the inclination angles derived from the axial ratios taken from the RC3 to initially restrict our sample to only face-on

[15] https://ps1images.stsci.edu/cgi-bin/ps1cutouts

[16] See §2.1 from Davis & Graham (2021) for further details.

($\theta \leq 30°$) galaxies, we elected to use our inclination angles that were derived during the process of measuring pitch angle.[17] As a result, some of our galaxies were subsequently found to have inclinations >30°, but we obtained more precise measurements. Our inclination estimates have a mean uncertainty of 3.°4, compared to 18.°5 for those from the RC3 axial ratios.[18] The $M_\bullet$–$v_{\rm max}$ and $M_\bullet$–ϕ relations are both determined from the same sample of galaxies, but the former exhibits a higher level of intrinsic scatter, $\epsilon = 0.45$ dex (equation 10 from Davis et al. 2019c).

3.3. *A Planar Black Hole Mass Scaling Relation*

Ever since the Magorrian et al. (1998) relation came onto the scene, the breadth and variety of black hole mass scaling relations has grown at a seemingly exponential rate in astrophysical literature. In our larger study (Jin & Davis 2023), we endeavored to use modern machine learning methods to try and identify higher-dimensional black hole mass scaling relations (*i.e.*, $M_\bullet$ plus *two or more* galactic parameters) that are more accurate predictors of black hole mass than some of the aforementioned two-dimensional black hole mass scaling relations (*i.e.*, $M_\bullet$ plus *one* galactic parameter).[19] For that study, we utilized a subfield of machine learning called symbolic regression (Cranmer 2023) to search for the best mathematical expressions to fit our dataset of dynamically-measured SMBH masses and their host galaxy parameters. The parent study of Jin & Davis (2023) identified an ideal (*i.e.*, optimally precise and simple) relationship among $M_\bullet$, ϕ, and $v_{\rm max}$ for spiral galaxies. We presented the details behind this trivariate relationship separately in Davis & Jin (2023).

From Davis & Jin (2023), the equation for the $M_\bullet$–ϕ–$v_{\rm max}$ relationship is:

$$\mathcal{M}_\bullet = \alpha(\tan|\phi| - 0.24) + \beta \log\left(\frac{v_{\rm max}}{211\,{\rm km\,s^{-1}}}\right) + \gamma, \quad (1)$$

with $\alpha = -5.58 \pm 0.06$, $\beta = 3.96 \pm 0.06$, $\gamma = 7.33 \pm 0.05$, and $\epsilon = 0.22 \pm 0.06$ dex in the $\mathcal{M}_\bullet$-direction, with parameters identified by `PySR` (Cranmer 2023) and refined via `Hyper-Fit` (Robotham & Obreschkow 2015, 2016). We utilize Equation 1 to predict black hole masses for all of our sample (see Column 11 of Table 1). Figure 1 illustrates a plot of the plane and the location of all 85 of our galaxies on the plane. The orientation of the plane conforms with expectations—**big** black holes reside in galaxies that have tightly wound spiral arms *and* whose disks are rapidly rotating, and **small** black holes are found in galaxies that have loosely wound spiral arms *and* whose disk are slowly rotating. The combination of these parameters is not surprising; Sarkar et al. (2023) find that later morphological types are primarily flocculent (in contrast to grand-design) galaxies with more loosely wound spiral arms and slower rotational velocities. For additional analyses and discussions, see Davis & Jin (2023) regarding the planar relation for spiral galaxies and Jin & Davis (2023) for higher-dimensional relations featuring all galaxy types.

We present a couple of metrics to help codify our best IMBH candidate host galaxies in the rightmost columns of Table 1. Column 12 displays the probability that the central black hole is an IMBH, *i.e.*, $P(\mathcal{M}_\bullet \leq 5)$ (via Davis & Graham 2021, equation 7). Column 13 provides the number of standard deviations below $10^5\,{\rm M}_\odot$, *i.e.*, $n\,\sigma = (5 - \mathcal{M}_\bullet)/\delta\mathcal{M}_\bullet$, which is equivalent to $P(\mathcal{M}_\bullet \leq 5)$, *e.g.*, $P(\mathcal{M}_\bullet \leq 5) = 68.3\% \equiv 1.0\,\sigma$. Together, we utilize these quality/qualifying parameters to categorize our sample into striations of likeliness that a galaxy is expected to harbor an IMBH.

Inclination (θ) is the one common source of error that affects both independent variables ($|\phi|$ and $v_{\rm max}$) in our study. Because of the small-angle approximation, an error in the inclination of a galaxy when it is close to face-on (0°) is more significant than an equally-sized error when a galaxy is close to edge-on (90°). This heteroscedasticity negatively affects the calculation of the intrinsic $v_{\rm max}$ from the observed line-of-sight velocity ($v_{\rm LOS}$), because $v_{\rm max} \equiv v_{\rm LOS} \csc\theta$. However, the opposite effect is applicable to the measurement of pitch angles. Because a galaxy must be artificially projected into a face-on orientation to measure pitch angle, galaxies that are already close to a face-on orientation require minimal modification. Specifically, the minor-axis length (b) of a galaxy is stretched to equal its major-axis length (a), *i.e.*, $a \equiv b \sec\theta$.

4. RESULTS

4.1. *Typical Central Black Hole in an Sd Galaxy*

[17] In fact, the act of determining inclination angles via the process of measuring pitch angles and/or Fourier transforms of spiral galaxy images has shown itself to be an accurate alternative to traditional inclination measurements via isophotal analysis (*e.g.*, Grosbøl 1985; Ma 2001; García-Gómez et al. 2004; Poltorak & Fridman 2007; Fridman & Poltorak 2010). Thus, reversing the procedure can yield precise inclination angle measurements of galaxies by adjusting the inclination angle until a galaxy's spiral structure is closely described by pure logarithmic spirals with ϕ such that the growth of the spirals (radius R as a function of galactocentric azimuth φ) is monotonic ($dR/d\varphi > 0$).

[18] From their study of uncertainties in the projection parameters of spiral galaxies, Barnes & Sellwood (2003) found systematic uncertainties of ≈4° in inclination derived from photometry due to the presence of nonaxisymmetric structures.

[19] Machine learning has also been utilized recently to try and identify globular clusters that host IMBHs (Pasquato et al. 2023).

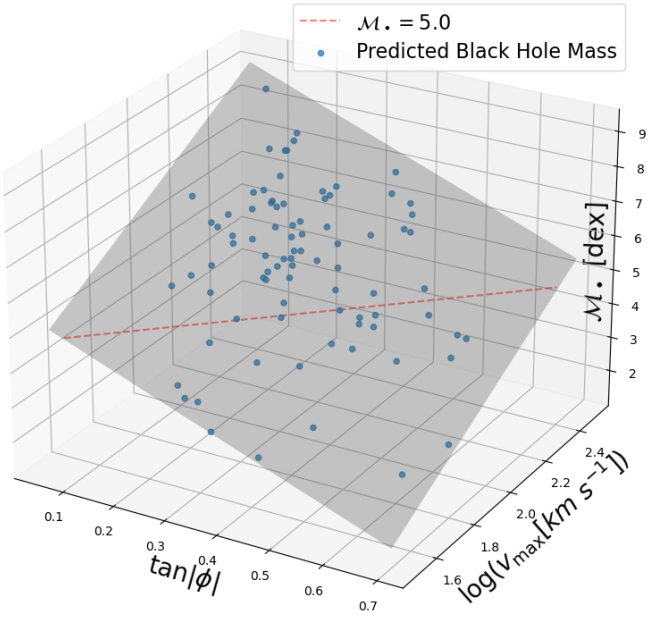

Figure 1. Here, we have reproduced the three-dimensional plot of the planar $M_\bullet$–ϕ–$v_{\rm max}$ relationship (Equation 1) from Davis & Jin (2023, figure 2). Onto the surface (◆), we show the locations of all 85 of our galaxies from this work (●) and a demarcation line (- - -) showing the boundary between supermassive and intermediate-mass black holes at $\mathcal{M}_\bullet = 5.0$. As shown, 23/85 of the galaxies lie below the dividing line, representing our IMBH-candidate host galaxies. Moreover, this enhanced plot illustrates that our galaxies are dispersed over the area of the plane, demonstrating a lack of degeneracy between the parameters by the apparent embedding of the two-dimensional manifold (*i.e.*, surface) in three-dimensional space. For an animation of this plot, see the following link, http://surl.li/kkjeu.

In Figure 2, we produce a histogram by summation of all 85 black hole mass estimates (determined by Equation 1) for our sample of 85 Sd galaxies. We then fit a skew-kurtotic-normal distribution to the histogram. In doing so, we find that the typical Sd galaxy hosts a black hole with $\mathcal{M}_\bullet = 6.00 \pm 0.14$, with $P(\mathcal{M}_\bullet \leq 5) = 27.7\%$. Expressed differently, this most probable mass of $(1.01 \pm 0.33) \times 10^6\,{\rm M}_\odot$ is $25.1\% \pm 8.2\%$ the mass of Sgr A* (Boehle et al. 2016).

Nominally, we expect that 1/3.61 of Sd galaxies harbor an IMBH. The RC3 provides morphological classifications for 17,801 diameter-selected galaxies, of which

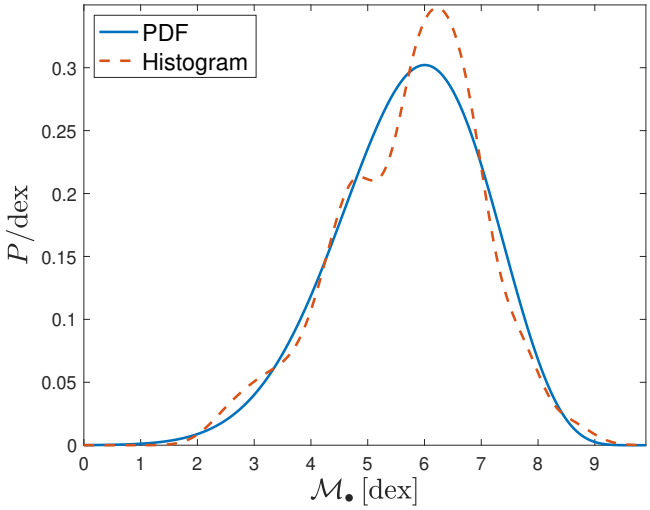

Figure 2. The distribution of black hole mass estimates ($\mathcal{M}_\bullet$) for the 85 Sd galaxies in our sample (from Column 11 of Table 1) has a mean $\mathcal{M}_\bullet$ of 5.73 ± 1.30 and a median of 5.89 ± 0.86. The smoothed histogram (- - -) is generated from the summation of all 85 mass estimates. The fitted PDF (——) for the Sd galaxies peaks at $\mathcal{M}_\bullet = 6.00 \pm 0.14$ (its mode). Here, the integrated probability under the PDF at $\mathcal{M}_\bullet \leq 5$ is 27.7%.

787 are classified as Sd, *i.e.*, 4.42%.[20] Given this frequency of Sd galaxies in our local Universe, we would, therefore, expect that >218 or >1.22%[21] of bright galaxies ($B_{\rm T} \lesssim 15.5\,{\rm mag}$) in our local Universe host an IMBH, *i.e.*, the "occupation fraction" (Zhang et al. 2009; Miller et al. 2015; Gallo & Sesana 2019). Using the cosmographic parameters from Planck Collaboration et al. (2020), this gives a comoving volume of $4.40 \times 10^7\,{\rm Mpc}^3$ for the RC3 extent and a lower limit

[20] A similar value of 3.92% (34/867) was found for Sd types by the diameter-selected sample of Lacerda et al. (2020). However, the magnitude-limited sample of the Carnegie-Irvine Galaxy Survey (Ho et al. 2011), plus the Milky Way, shows only 9/606 galaxies (1.49%) are type Sd, whereas its magnitude- and volume-limited subsample shows only 1/208 galaxies (0.48%) are type Sd (Davis et al. 2014; Mutlu-Pakdil et al. 2016). The EFIGI catalogue (Baillard et al. 2011) is a subset of 4,458 galaxies from the RC3, but no longer considers peculiar galaxies or galaxies with special features as belonging to separate stages. Thus, they classify an even higher fraction (285/4,458 = 6.39%) of galaxies as $T = 7$ (de Lapparent et al. 2011). It is worth noting that there is an even higher fraction (*i.e.*, almost double) of Sd galaxies in the nearby Universe; there are 39 Sd galaxies out of 454 galaxies with a classification (8.6%) in the RC3 at $cz < 1{,}000\,{\rm km\,s^{-1}}$ ($z < 0.003$; luminosity distances out to $d = 15\,{\rm Mpc}$). This could indicate a real local excess or maybe a bias against Sd identification in more distant galaxies.

[21] This is a lower limit because we are not accounting here for other potential hosts of IMBHs (*e.g.*, dwarf galaxies and globular clusters) or their frequency (albeit, to a lesser extent) in earlier type spirals.

for the number density of central IMBHs in our local Universe $>4.96 \times 10^{-6}\,\mathrm{Mpc}^{-3}$.

4.2. *Additional Observational Data*

4.2.1. *BPT Classifications*

We consulted the Reference Catalog of galaxy SEDs (RCSED; Chilingarian et al. 2017) to obtain nuclear classifications for each galaxy. The RCSED database utilizes the Baldwin-Phillips-Terlevich (hereafter BPT; Baldwin et al. 1981) [N II]/Hα versus [O III]/Hβ standard optical diagnostic classification, according to Kewley et al. (2006).[22] As such, galaxies are classified as containing an H II-region, AGN, or both (composite). Only one galaxy (UGC 8171) is classified as having a *bona fide* AGN,[23] and another is a composite (UGC 4622). Coincidentally, both galaxies are predicted to have similar black hole masses (UGC 4622: $\mathcal{M}_\bullet = 6.16 \pm 0.46$, with $P(\mathcal{M}_\bullet \leq 5) = 0.6\%$; UGC 8171: $\mathcal{M}_\bullet = 6.55 \pm 0.39$, with $P(\mathcal{M}_\bullet \leq 5) \approx 0.0\%$), which are strongly inconsistent with being IMBHs.

Fourteen galaxies (including the composite UGC 4622) are classified as H II-region-like galaxies. The sample peak probability (mode) black hole mass for these 14 galaxies is $\mathcal{M}_\bullet = 5.14 \pm 0.35$, with $P(\mathcal{M}_\bullet \leq 5) = 36.0\%$. Therefore, these 14 H II-region-like galaxies have a slightly higher probability of containing central IMBHs than the typical Sd galaxy. A possible explanation for this difference could emerge from varied gas fractions between these subpopulations of galaxies (see a further discussion in §5.1).

4.2.2. *Nuclear X-ray Point Sources*

We checked the CXO archive for observations of all galaxies in our sample. The CXO has observed eight of our galaxies; however, only one galaxy (NGC 2500) exhibited a measurable flux of X-ray photons emanating from its nucleus. With $\mathcal{M}_\bullet = 5.57 \pm 0.70$ and $P(\mathcal{M}_\bullet \leq 5) = 20.7\%$, NGC 2500 has a slightly higher probability of possessing an IMBH than the typical Sd galaxy. The seven galaxies without a measurable nuclear X-ray source have a sample mode black hole mass of $\mathcal{M}_\bullet = 5.79 \pm 0.41$, *but* $P(\mathcal{M}_\bullet \leq 5) = 41.4\%$ with a strong tail towards lower masses. Thus, these seven galaxies, where X-ray sources have been sought (but not found), are exactly *twice* as likely to harbor an IMBH in their nuclei (as compared to NGC 2500). Put another way, finding a nuclear X-ray source implies that a galaxy is twice as likely to harbor an SMBH, instead of an IMBH. Therefore, non-detection of nuclear X-ray sources could be a useful diagnostic for identifying IMBH host galaxy candidates.

This paltry harvest of nuclear X-ray sources for our sample is not unexpected, because we deliberately selected intrinsically faint Sd galaxies. With average black holes masses less than a million solar masses and Eddington ratios of $\sim 10^{-6}$, the typical Sd galaxy will likely have weak or no AGN signature. Also, Sd galaxies presumably lack one alleged mechanism behind AGN triggering, *i.e.*, major mergers.[24] Optical emission line diagnostic tests for activity and/or X-ray emission from nuclei are usually reliable indications for the presence of an accreting SMBH. However, the lack of such indicators from the centers of Sd galaxies is not evidence for the lack of black holes, which may be in a quiescent phase of their duty cycles.

The occupation fraction of galaxies with nuclear X-ray emission can be quite different, depending on the sample selection. For example, Williams et al. (2022) found X-ray emission coincident within 2″ of their optical galaxy centers in the majority of their galaxies ($150/213 = 70.4\%$). Whereas, Nwaokoro et al. (2021) found X-ray sources within 3″ of their host galaxy centers in only a tiny fraction of their sample ($7/1200 = 5.83‰$). The difference being that the former sample (Williams et al. 2022) was constructed as a statistically complete sample of nearby galaxies, while the latter sample (Nwaokoro et al. 2021) is a sample of only low-mass galaxies ($M_{\mathrm{gal},\star} \lesssim 10^{9.5}\,\mathrm{M}_\odot$). Moreover, Ohlson et al. (2023) found that in low-mass late-type galaxies X-ray fractions are lower and positional offsets of X-ray detections from their galactic centers are higher (possibly due to increased astrometric uncertainty). Thus, in general, exceedingly few X-ray sources exist in low-mass galaxies.

[22] As Birchall et al. (2022) point out, the BPT diagnostic clearly fails at reliably identifying sources as AGNs in lower mass galaxies. Moreover, emission line flux ratio diagnostics can fail to identify entire subpopulations of AGNs when applied to single-fiber optical spectra (Comerford et al. 2022). Other diagnostics, such as He II, may be better suited to detecting ionizing photons from AGNs in low-metallicity, star-forming dwarf galaxies (Umeda et al. 2022; Tozzi et al. 2023).

[23] For comparison, Lacerda et al. (2020) found that none of the 34 Sd galaxies in their sample possess an AGN.

[24] Models suggest that major mergers may establish galaxy-wide, gravitationally-induced torques that drive gas toward a galactic center, which may set off an AGN (*e.g.*, Hopkins et al. 2006). However, the jury is decidedly hung when it comes to reaching a verdict about whether major mergers are relevant (*e.g.*, Koss et al. 2010; Ellison et al. 2011; Hong et al. 2015; Weston et al. 2017; Goulding et al. 2018; Gao et al. 2020; Hernández-Toledo et al. 2023; Breiding et al. 2023) or not (*e.g.*, Cisternas et al. 2011; Kocevski et al. 2012; Karouzos et al. 2014; Villforth et al. 2019; Lambrides et al. 2021) in triggering AGN.

Moreover, an IMBH might not reside at the center of a galaxy. Due to their diminished mass, IMBHs traverse a difficult path sinking to the centers of their host galaxies and are more prone to wander away (Binggeli et al. 2000; Bellovary et al. 2019, 2021; Barrows et al. 2019; Pfister et al. 2019; Reines et al. 2020; Mezcua & Domínguez Sánchez 2020; Ma et al. 2021; Ricarte et al. 2021; Di Cintio et al. 2023; Partmann et al. 2023) as compared to their more massive SMBH cousins.[25] In particular, perhaps the best (and most studied) IMBH candidate is HLX-1, which is 3.7 kpc from the center of ESO 243-49: (Farrell et al. 2009, 2012; Soria et al. 2010, 2011, 2012, 2013; Webb et al. 2010, 2012, 2017).[26] However, Weller et al. (2023b) and Di Matteo et al. (2023b) remark about the largely-missing population of wandering IMBHs, which rarely reveal themselves in the hyper-luminous X-ray sources (HLXs) regime. IMBHs may also be associated with the merging remnants of dwarf galaxies onto larger galaxies (Webb et al. 2010, 2017; Farrell et al. 2012; Mapelli et al. 2012b; Soria et al. 2013; Mezcua et al. 2015; Kim et al. 2015, 2017, 2020; Graham et al. 2021a).

4.3. *IMBH Targets of Interest*

We define a target of interest to have $P(\mathcal{M}_\bullet \leq 5) > 50\%$ ($n\,\sigma > 0$). Looking down Table 1 Column 12, we identify 23 targets of interest (points plotted below the dashed red line in Figure 1). Indeed, this fraction of galaxies (23/85=27.1%) is comparable with the $P(\mathcal{M}_\bullet \leq 5) = 27.7\%$ value we obtain from Figure 2. For these 23 galaxies, we wager that the odds are favorable that they each host a central IMBH. Among these targets, UGC 1544 is our most likely example to host an IMBH, with an expected mass of only $323 \pm 293\,\mathrm{M}_\odot$. Moreover, these 23 galaxies are all relatively nearby; their mean distance is 55.2 ± 29.2 Mpc, median distance is 52.5 ± 18.2 Mpc, and a peak probability distance of 42.1 ± 6.1 Mpc. Thus, these galaxies pose appealing targets for further study.

4.3.1. *Targets with Additional Consideration*

UGC 3826 possesses an NSC with a mass of $\mathcal{M}_{\mathrm{NSC},\star} = 6.04 \pm 0.09$ (Georgiev & Böker 2014; Georgiev et al. 2016). By application of the $M_\bullet$–$M_{\mathrm{NSC},\star}$ relation (Graham 2020, equation 9), we predict a black hole mass of $\mathcal{M}_\bullet = 3.53 \pm 0.95$, with $P(\mathcal{M}_\bullet \leq 5) = 93.9\%$. Additionally, we can apply the $M_\bullet$–$M_{\mathrm{gal},\star}$ relation (Davis et al. 2018, equation 3) to the total stellar mass of UGC 3826 ($\mathcal{M}_{\mathrm{gal},\star} = 9.33 \pm 0.27$) and predict a black hole mass of $\mathcal{M}_\bullet = 2.75 \pm 1.30$, with $P(\mathcal{M}_\bullet \leq 5) = 95.8\%$. As we can see, these black hole mass predictions are very consistent with the value we found from Equation 1, $\mathcal{M}_\bullet = 3.40 \pm 0.60$, with $P(\mathcal{M}_\bullet \leq 5) = 99.6\%$.

Additionally, we identified two of our galaxies with black hole mass estimates via the $M_\bullet$–$\mathcal{C}_{\mathrm{FUV,tot}}$ and $M_\bullet$–$\mathcal{C}_{\mathrm{NUV,tot}}$ relations of Dullo et al. (2020), where $\mathcal{C}_{\mathrm{FUV,tot}}$ is the total FUV$-[3.6\,\mu\mathrm{m}]$ color and $\mathcal{C}_{\mathrm{NUV,tot}}$ is the total NUV$-[3.6\,\mu\mathrm{m}]$ color.[27] For **UGC 8153**, Dullo et al. (2020) predict $\mathcal{M}_\bullet = 4.89 \pm 0.85$, with $P(\mathcal{M}_\bullet \leq 5) = 55.1\%$, and $\mathcal{M}_\bullet = 4.59 \pm 0.85$, with $P(\mathcal{M}_\bullet \leq 5) = 68.5\%$, from $\mathcal{C}_{\mathrm{FUV,tot}}$ and $\mathcal{C}_{\mathrm{NUV,tot}}$, respectively. Also, we can apply the $M_\bullet$–$M_{\mathrm{gal},\star}$ relation (Davis et al. 2018, equation 3) to the total stellar mass of UGC 8153 ($\mathcal{M}_{\mathrm{gal},\star} = 9.78 \pm 0.16$) and predict a black hole mass of $\mathcal{M}_\bullet = 4.11 \pm 0.98$, with $P(\mathcal{M}_\bullet \leq 5) = 81.7\%$. Thus, the color-based and total stellar mass predictions for UGC 8153 are consistent with our predictions for an IMBH, $\mathcal{M}_\bullet = 4.13 \pm 0.55$, with $P(\mathcal{M}_\bullet \leq 5) = 94.4\%$.

Similarly for **UGC 10020**, Dullo et al. (2020) predict $\mathcal{M}_\bullet = 5.46 \pm 0.85$, with $P(\mathcal{M}_\bullet \leq 5) = 29.4\%$, and $\mathcal{M}_\bullet = 5.35 \pm 0.85$, with $P(\mathcal{M}_\bullet \leq 5) = 34.1\%$, from $\mathcal{C}_{\mathrm{FUV,tot}}$ and $\mathcal{C}_{\mathrm{NUV,tot}}$, respectively. Furthermore, we can apply the $M_\bullet$–$M_{\mathrm{gal},\star}$ relation (Davis et al. 2018, equation 3) to the total stellar mass of UGC 10020 ($\mathcal{M}_{\mathrm{gal},\star} = 9.59 \pm 0.22$) and predict a black hole mass of $\mathcal{M}_\bullet = 3.55 \pm 1.14$, with $P(\mathcal{M}_\bullet \leq 5) = 89.9\%$. Likewise, the color-based total stellar mass predictions for UGC 10020 are consistent with our predictions for an IMBH, $\mathcal{M}_\bullet = 4.98 \pm 0.47$. However, the higher color-based mass predictions for UGC 10020 are in line with our weak $P(\mathcal{M}_\bullet \leq 5) = 52.0\%$, which is the least certain IMBH candidate among our sample of 23 targets of interest.

5. DISCUSSION

5.1. *The Prototypical Sd Galaxy*

We observe that the geometry of the spiral arm shape in Sd galaxies is not always as loosely wound as one might expect. Some of this is due to obvious misclas-

[25] However, Chu et al. (2023) point out that off-center SMBHs are common in brightest cluster galaxies due to numerous galaxy mergers in their history, in which, an SMBH can become significantly kicked out of the galactic center via dynamical interactions. Such offset SMBHs could potentially be detected via distortions that they cause in gravitational lens galaxies (Piro et al. 2023a; Giani et al. 2023).

[26] See also, the much-discussed ultra-luminous source from a possible IMBH in Messier 82 (Patruno et al. 2006; Muxlow et al. 2010; Joseph et al. 2011; Pasham et al. 2014).

[27] As expected, the $M_\bullet$–$\mathcal{C}$ relations from Dullo et al. (2020) are such that more massive black holes reside in redder galaxies. Similarly, Baker et al. (2023) found that more massive black holes reside in galaxies with higher metallicities.

sifications of the morphological type.[28] For example, our smallest pitch angle measurement is $|\phi| = 5.^{\circ}8 \pm 2.^{\circ}8$ for UGC 1702, which is an absurdly small pitch angle for a legitimate Sd galaxy. However, UGC 1702 is also one of the most massive galaxies in our sample, with $\mathcal{M}_{\rm gal,\star} = 10.55 \pm 0.21$. Moreover, it has a high rotational velocity with $v_{\rm max} = 283.8 \pm 14.3\,{\rm km\,s^{-1}}$. Indeed, our trivariate relation predicts the most massive SMBH in our sample, with a mass of $\mathcal{M}_{\bullet} = 8.61 \pm 0.37$, with $P(\mathcal{M}_{\bullet} \leq 5) \approx 0.0\%$.

In some instances, the geometry of arms may not agree well with a weak bulge. The RC3 bases their classifications on the de Vaucouleurs (1959) classification approach, which is based the appearance of the spiral arms and the bulge of a galaxy. They consider both (*i*) the degree of openness (*i.e.*, $|\phi|$) and (*ii*) the resolution of spiral arms into star clusters or very luminous stars (*i.e.*, knotty vs. smooth spiral structure), and additionally (*iii*) the relative prominence of the bulge or central concentration (*i.e.*, B/T).[29] These criteria that govern the stage for spirals may be inconsistent in some cases or may be overruled by other factors that affect the morphological type (Sandage 1961; Sandage & Bedke 1994). Importantly for our study of Sd types, Mengistu & Masters (2023) find that bluer and lower mass galaxies most closely follow the "expected" arm windiness correlation with bulge size, *i.e.*, smaller bulges with loosely wound spiral arms.

The B/T ratio is directly related to the morphological type, in general, but with considerable scatter for a given type (Simien & de Vaucouleurs 1986; Laurikainen et al. 2007; Graham & Worley 2008; Willett et al. 2013). Specifically, Masters et al. (2019) find that galaxies with larger bulges favor tighter spiral arms, while those with smaller bulges have a wide range of arm winding; *cf.* Lingard et al. (2021), who find no correlation between bulge size and pitch angle. Very recently, Chugunov et al. (2023) affirmed "that the pitch angle of spiral arms decreases with increasing bulge or bar fraction." Smith et al. (2022) found that blue (*i.e.*, star-forming) galaxies predominantly exhibit loosely wound spiral arms and red (*i.e.*, quiescent) galaxies mainly display tightly wound spiral arms. Similarly, late-type spirals have been shown to have stronger arms (Yu & Ho 2020) and higher star-formation rates (Yu et al. 2021).[30]

Importantly, multiple studies find a general trend (albeit with considerable scatter) between pitch angle and Hubble stage, *i.e.*, $|\phi| \propto T$ (Kennicutt 1981; Seigar & James 1998; Ma et al. 1999; Baillard et al. 2011; Yu et al. 2018; Díaz-García et al. 2019; Yu & Ho 2019, 2020; Chugunov et al. 2023). More precisely, Treuthardt et al. (2012) show that the correlation between $|\phi|$ and T is tightest when selecting spiral galaxies with fast rotating bars, which is in close agreement with the theoretical relation (Roberts et al. 1975). Notably, Yu & Ho (2019) find that $|\phi|$ is most closely correlated with $M_{\rm gal,\star}$, especially so for low-mass galaxies. Overall, there are related connections between multiple parameters, with positive correlations between ϕ–T and ϕ–(absolute magnitude) relations (Kennicutt 1981), and negative correlations between ϕ–$v_{\rm max}$ (Kennicutt 1981; Davis et al. 2019c) and $v_{\rm max}$–T (Roberts 1978) relations.

Frustratingly, if the image resolution is inadequate, the degree of openness cannot be accurately determined, and the default is toward a later type. Indeed, Peng et al. (2018) empirically found that $|\phi| \propto z$, that is, the average pitch angle observed in galaxies is perceived to increase (loosen) as a function of redshift. Although, this is not expected to be an intrinsic effect, but rather a systematic effect of "tightly wound arms becoming less visible as image quality degrades" (Peng et al. 2018). Hence, some of the more distant galaxies in our sample of "Sd" galaxies could have tightly wound spiral arms that were not accounted for in classification catalogs from decades ago due to lower image resolutions. From that point of view, the ($T = 7.0$) morphological types for our sample could be considered upper limits. Additionally, Graham & Worley (2008) point out that disk luminosities become progressively dimmer with increasing Hubble type, further exacerbating efforts to resolve the geometry of spiral arms. As telescope technology continues to advance, it becomes increasingly probable that new, high-resolution surveys may overturn old morphological classifications if they can better resolve the geometry of the spiral arms.

[28] Consulting the meta-analysis of morphological types for our galaxies from HyperLeda, we find that only two of our galaxies have morphological types that do not agree ($T \neq 7$) with our adopted classifications from the RC3: UGC 283, $T = 5.8 \pm 0.7$ and UGC 10146, $T = 8.7 \pm 1.4$.

[29] Willett et al. (2013) and Masters et al. (2019) argue that modern morphological classifications of spiral galaxies have devolved the traditional tenets of the classic Hubble-Jeans sequence (Jeans 1919, 1928; Lundmark 1925; Hubble 1926a,b, 1927, 1936) that prioritized spiral arm winding (van den Bergh 1998; de Lapparent et al. 2011), but still considered bulge size; contemporary morphological sequences are now predominantly ordered on central bulge size alone, with no reference to spiral arms (Graham & Worley 2008; Willett et al. 2013).

[30] Aktar et al. (2023) find no evidence of a trend between star-formation rates and pitch angle, but postulate that the lack of a correlation "may be explained by different star formation efficiencies caused by the distinct galactic ambient conditions."

Even though the Sd sample tends towards large pitch angles, the broad range they cover could be a possible indication of their diverse origins or evolutionary histories. The gas content in Sd galaxies[31] could also have a role to play in diminished pitch angle values. Davis et al. (2015) observed that, due to spiral density wave theory (*i.e.*, Lin & Shu 1966), the pitch angle of spiral galaxies is due to both the central mass of a galaxy (which includes the central black hole), as well as the density of the disk of a galaxy, such that the pitch angle is directly proportional to the disk density and inversely proportional to the central mass. Graham & Worley (2008) show that the surface density of disks decrease as the morphological type of a galaxy becomes increasingly later.[32] Thus, if the ratio of disk density to central mass does not decrease at the same rate as the morphological type increases, the pitch angle of an Sd galaxy could very well be lower than expected if it were only due to the central mass.[33] Therefore, our pitch angle measurements could be skewing the predicted black hole masses towards higher masses in some cases, depending on the influence of unknown densities.[34] Notably, Hart et al. (2017) found that central mass concentration alone does not govern pitch angle; they found that galaxies which are more disk dominated contain more spiral arms with tighter pitch angles.

It is also notable that there appears to be an empirical correlation between pitch angle and dark matter halos; Seigar et al. (2005, 2006, 2014) have demonstrated an anticorrelation between pitch angle and the central mass concentration of a spiral galaxy via measurement of the rate of shear of its rotation curve (Γ).[35] Additionally, simulations have shown that late-type bulgeless galaxies pose an enigma due to an apparent dichotomy between their observed and simulated angular momenta. D'Onghia & Burkert (2004) demonstrated that in the absence of major mergers, dark matter halos have too low an angular momentum to reconcile the observed disks of their embedded bulgeless late-type galaxies. Indeed, Rodriguez-Gomez et al. (2022) found that galaxies with higher specific angular momenta reside in faster spinning halos and tend to host less massive black holes. Also, Rodriguez-Gomez et al. (2022) further described that halo spin is anti-correlated with black hole mass at fixed galaxy or halo mass. Such complications could be an additional factor in discrepancies between our observed properties (*i.e.*, pitch angle, stellar mass, and rotational velocities). This further warrants and justifies our adoption of a higher-dimensional black hole mass predictor, rather than relying on only one two-dimensional scaling relation parameterization (see also Williams et al. 2023b).

Overall, we find that the notion of a truly average Sd galaxy is false. Similarly, Daniels (1952) found, in his landmark anthropometric study, that the *average man* does not exist. From a study of 4,063 men, Daniels (1952) found that no man was average (*i.e.*, within ±0.3 standard deviations of the mean) across more than nine out of the 132 body measurements performed for the study. Using the same definition of average, we find that only three of our 85 galaxies are "average" across $|\phi|$, $v_{\rm max}$, and $\mathcal{M}_{\rm gal,\star}$. These most average galaxies include: UGC 384, 2109, and 3074. Together, these three prototypical Sd galaxies have a modal $\mathcal{M}_\bullet = 5.84\pm0.19$, with $P(\mathcal{M}_\bullet \leq 5) = 0.3\%$. Therefore, IMBHs are likely to be harbored only in Sd galaxies that are significantly looser wound, rotating slower, and/or less massive than the exemplar of Sd galaxies.

[31] Lacerda et al. (2020) found that Sd galaxies have some of the highest gas fractions ($f_{\rm gas}$) of any morphological type (see their figure 9 and table 3), with an average $f_{\rm gas} = 6.76\%$, which is almost three times the average proportion they found in their Sa galaxies ($f_{\rm gas} = 2.40\%$).

[32] This can become problematic in accounting for later morphological types in the galaxy stellar mass function; Kim et al. (2023) estimate that the majority of low-surface brightness galaxies are missed in redshift surveys at $z > 0.9$. Indeed, the problem is not easily ignorable since the number density of galaxies *increases* monotonically as their stellar masses *decrease* (Driver et al. 2022). Moreover, the prominence of low stellar-mass galaxies becomes increasingly relevant as the slope of the galaxy stellar mass function is shown to steepen with redshift (Navarro-Carrera et al. 2023).

[33] Another complication to consider is the environment of each galaxy. Cluster galaxies can experience ram-pressure stripping, which "unwinds" their spiral arms (Bellhouse et al. 2021). Although, this effect would act to loosen (*i.e.*, increase $|\phi|$) the pitch angle of a galaxy.

[34] We are also cognizant of the possibility that other spiral genesis mechanisms besides the spiral density wave theory could be at play, *e.g.*, swing amplification (see Dobbs & Baba 2014, for a review). Notably, Hart et al. (2018) found that ≈40% of the galaxies in their sample have spiral arms that can be modeled by swing amplification. Yu & Ho (2020) compared their work with the models of Hart et al. (2018) and speculated that later morphologically-typed spiral galaxies in their sample could be similarly influenced by swing amplification. Following work by Yu & Ho (2018) and Pringle & Dobbs (2019), Lingard et al. (2021) found that their sample of spiral galaxies could be explained by evolution of transient/recurrent spirals via swing amplification that wind up over time, *if* pitch angles are sufficiently high. Similarly, Reshetnikov et al. (2022) showed from observations that $|\phi| \propto z$, *i.e.*, pitch angles tend to decrease (windup) with time.

[35] We note that subsequent studies (Kendall et al. 2015; Yu et al. 2018; Yu & Ho 2019) have also found an anticorrelation between $|\phi|$ and Γ, albeit a much weaker anticorrelation with higher scatter.

5.2. *Sd Classifications: Optical vs. Mid-IR*

In order to draw comparisons of our population of Sd galaxies, we sought an independent study that had a statistically viable number of Sd galaxies with quantitative pitch angle measurements. The largest such sample we could find comes from the *Spitzer* Survey of Stellar Structure in Galaxies (Sheth et al. 2010, hereafter S^{4}G). A series of papers (Buta et al. 2010, 2015) goes through careful morphological classifications of their 2,352 galaxies. Using the classifications of Buta et al. (2015) and pitch angle measurements by Herrera-Endoqui et al. (2015), refined by Díaz-García et al. (2019), we identified 22 Sd galaxies with pitch angle measurements from the S^{4}G sample.

In Figure 3, we present a comparison of the pitch angle distribution of our 85 Sd galaxies alongside the 22 Sd galaxies from Díaz-García et al. (2019). Both distributions demonstrate a similar shape (*i.e.*, positive skewness), but the peaks are notably different: $|\phi| = 16.^\circ0 \pm 0.^\circ8$ for our galaxies and $|\phi| = 19.^\circ8 \pm 2.^\circ0$ for the galaxies from the S^{4}G sample. We performed a Kolmogorov–Smirnov (K–S) test (Kolmogorov 1933; Smirnov 1948) to assess the likelihood that both samples come from the same distribution. In doing so, we found a p-value = 0.0110, thus rejecting the null hypothesis at the 1.10% level (*i.e.*, a 98.90% probability that the samples come from different parent populations).

However, this is not the end of the story for this comparison. Crucially, our 85 galaxies were classified as Sd galaxies by the RC3 based on B-band images, whereas the 22 galaxies classified as Sd galaxies by Buta et al. (2015) were based on middle-infrared (mid-IR) images. Specifically, Buta et al. (2015) exclusively used 3.6-μm images, which highlight the photospheric light of old stars (Pahre et al. 2004). This can lead to a complicated difference in the perceived morphologies that were traditionally observed in B-band light that highlights young stellar populations and is strongly affected by extinction and reddening. Moreover, Buta et al. (2015) also used an updated morphological notation system (*e.g.*, Buta 2014) that is similar to, but more extensive than, the notational system provided in the RC3.

Overall, it is generally accepted that the morphological classification schemes derived from B-band observations can be effectively applied to infrared images and reproduce the gamut of morphological diversity (Eskridge et al. 2002; Buta et al. 2010, 2015). However, it has been claimed that optical and near-IR morphologies of spiral galaxies are uncorrelated; Block & Puerari (1999) found that "the Hubble tuning fork does not constrain the morphology of the old stellar Population II disks." Moreover, Block & Puerari (1999) found extreme examples where galaxies on opposite ends of the Hubble tuning fork in optical light can have the same morphology when observed in the near-infrared (K'-band). Nonetheless, Eskridge et al. (2002) found that B-band vs. H-band morphologies are mostly similar. Separately, Buta et al. (2010, 2015) found that B-band vs. 3.6-μm morphologies are also largely the same. Although, systematic differences are observed.[36]

Infrared morphologies exhibit a clear "earlier effect" (Eskridge et al. 2002; Buta et al. 2010, 2015), which is a result of the increased prominence of the bulge and the decreased prominence of star-forming regions in spiral

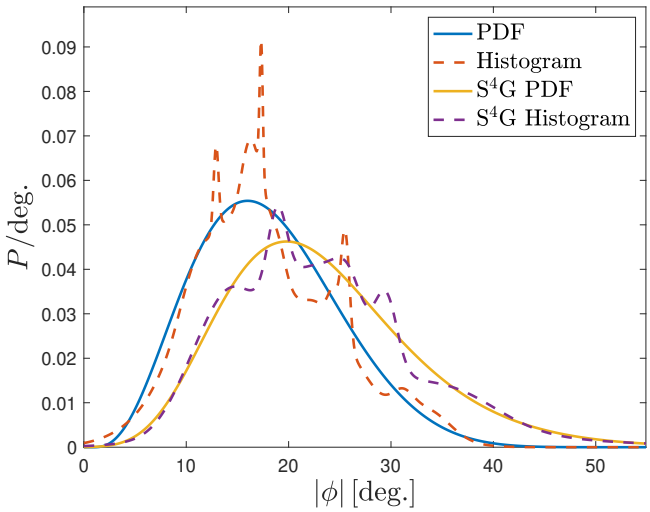

Figure 3. The distribution of the pitch angles ($|\phi|$) for our sample of 85 Sd galaxies (from Table 1, Column 6) with a mean $|\phi|$ of $18.^\circ0 \pm 7.^\circ0$ and a median of $17.^\circ1 \pm 4.^\circ7$. The smoothed histogram (- - -) is generated from the summation of all 85 pitch angle measurements. The fitted PDF (——) peaks at $|\phi| = 16.^\circ0 \pm 0.^\circ8$. We compare this with a sample of 22 Sd galaxies (- - -) with pitch angle measurements from the S^{4}G sample (Herrera-Endoqui et al. 2015; Díaz-García et al. 2019), with a mean $|\phi|$ of $23.^\circ3 \pm 9.^\circ4$, a median of $22.^\circ2 \pm 6.^\circ0$, and a fitted PDF (——) that peaks at $|\phi| = 19.^\circ8 \pm 2.^\circ0$.

[36] For a further investigation of how pitch angle measurements vary as a function of the wavelength of light and comparisons with predictions of the density wave theory, see the following papers (*e.g.*, Pour-Imani et al. 2016; Yu et al. 2018; Miller et al. 2019; Abdeen et al. 2020, 2022; Martínez-García et al. 2023; Chen et al. 2023c).

arms when observed in the infrared.[37] Thus, because the bulges visually stand out more in IR images, they tend to be classified as an earlier type than they were in B-band images. Specifically, Eskridge et al. (2002) find that their H-band classifications are systematically one stage earlier than the RC3 B-band classifications on average ($T_H = T_B - 1$). Therefore, it is plausible that the 22 S^{4}G $T_{3.6\,\mu\mathrm{m}} = 7$ galaxies that we compare with in Figure 3 are actually $T_B = 8$ galaxies with expectedly higher pitch angles, whose classifications are being overruled by their more prominent bulges when observed in the mid-IR.

We identified one of the 22 S^{4}G galaxies (NGC 5668) also in our sample that was independently measured by Herrera-Endoqui et al. (2015) and Díaz-García et al. (2019). Díaz-García et al. (2019) measured a pitch angle of $|\phi| = 29\overset{\circ}{.}7 \pm 3\overset{\circ}{.}9$, which is slightly higher, but consistent with our determination of $|\phi| = 27\overset{\circ}{.}3 \pm 2\overset{\circ}{.}8$ for NGC 5668. However, Buta et al. (2015) classify NGC 5668 as SAB(rs)cd, or $T_{3.6\,\mu\mathrm{m}} = 6.5$. Thus, supporting our suspicions of the earlier effect in its classification, although the pitch angles remain consistent in this case. When ultimately analyzed in aggregate, the statistically-significant observation of larger absolute pitch angles for the 3.6-μm sample confirms the implications of our aforementioned K–S test that the samples are drawn from different populations. Verily, comparison of morphologies across the electromagnetic spectrum is problematic and confounds demographical comparisons of galaxies.

5.3. *Comparison with a General Spiral Population*

In their study of a volume- and magnitude-limited sample of 140 spiral galaxies, Davis et al. (2014) found that the black hole mass function (BHMF) of spiral galaxies peaks at $1.17 \times 10^7\,\mathrm{M}_\odot$. Their volume-limited sample of 140 spiral galaxies is comprised of Sa, Sab, Sb, Sbc, Sc, Scd, Sd, and Sm types. However, it included only one (1%) Sd galaxy (ESO 138-010); the most common morphological type was Sc (34%; see their figure 3).

For comparison with their BHMF, we have produced a distribution of our black hole mass estimates (Figure 2).[38] From Figure 2, we find that the black hole mass distribution of Sd galaxies is indeed significantly different from the general spiral galaxy sample of Davis et al. (2014, their figure 7). Our fitted PDF peaks at $1.01 \times 10^6\,\mathrm{M}_\odot$, or 8.63% of the most probable black hole mass found in an average (Sc) spiral galaxy.

We also present the distributions of pitch angles (Figure 3), rotational velocities (Figure 4), and total stellar masses (Figure 5). As we can see, these distributions exhibit slight telltale evidence of multiple populations also reflected by the multimodal distribution of predicted black hole masses in Figure 2. These similarities across independent measurements give credence to the seemingly disparate spiral geometries uncovered by our pitch angle measurements across this sample of only Sd galaxies.[39] We note that our general PDF fit to the pitch angle distribution in Figure 3 is not appreciably different from the general shape of the distribution for all spiral types (Davis et al. 2014, figure 6).[40] However, the histogram for Sd galaxies in Figure 3 does exhibit a subpopulation of high pitch angle galaxies (*e.g.*, the prominence at $|\phi| = 25\overset{\circ}{.}5$), and lacks the enhanced population of galaxies with $|\phi| \lesssim 10^\circ$ found in Davis et al. (2014). This result is also reflected in the recent work of Fusco et al. (2022), who conducted a follow-up study to Davis et al. (2014) by analyzing the complementary population of 74 low-mass galaxies (peak probability at $|\phi| = 17\overset{\circ}{.}5$) that was excluded from Davis et al. (2014). Fusco et al. (2022) report a similar enhancement to the BHMF from Scd–Sm galaxies, and show that galaxies in this morphological population are predominantly the hosts of "less-than-supermassive" black holes ($M_\bullet \lesssim 10^6\,\mathrm{M}_\odot$).

5.4. *Implications*

5.4.1. *Seeding Models*

One of the most challenging conundrums at the frontier of astrophysics is how SMBHs formed in less than 1 Gyr ($z > 6$). SMBHs upwards of $\sim 10^9\,\mathrm{M}_\odot$ (hosted in stellar bulges of $\sim 10^{10}\,\mathrm{M}_\odot$; Tripodi et al. 2023) have been identified in observations of quasars at $z > 6$ (Fan

[37] Indeed, the extensive multi-wavelength bulge-disk decomposition study of M81 (NGC 3031) by Gong et al. (2023) showed that the Sérsic index (Sersic 1968) and effective radius of its bulge are proportional to wavelength, so much so that M81 appears to have a prominently classical bulge in the infrared and bulgeless at ultraviolet wavelengths. However, Ito et al. (2023) saw a negative correlation between the observed wavelength and effective radius of $z \geq 3$ quiescent galaxies, and their resulting size–mass relation is lower than those observed at lower redshifts (*e.g.*, van der Wel et al. 2014; Hon et al. 2022, 2023). See also Yao et al. (2023), Ono et al. (2023), and Ormerod et al. (2023), for their studies of the variation of morphological parameters with rest-frame wavelength.

[38] In this and subsequent figures, the histograms are the summation of individual normal distributions that describe each measurement.

[39] See also the recent meta-analysis performed by Savchenko et al. (2020), whose figure 13 demonstrates significant variance of pitch angle across morphological types.

[40] The modes of both the distributions for Sd ($|\phi| = 16\overset{\circ}{.}0$) and all ($|\phi| = 18\overset{\circ}{.}5$) spiral galaxies are remarkably close to the pitch angle ($|\phi| \approx 17\overset{\circ}{.}0$) of the golden spiral (Davis et al. 2014, appendix A).

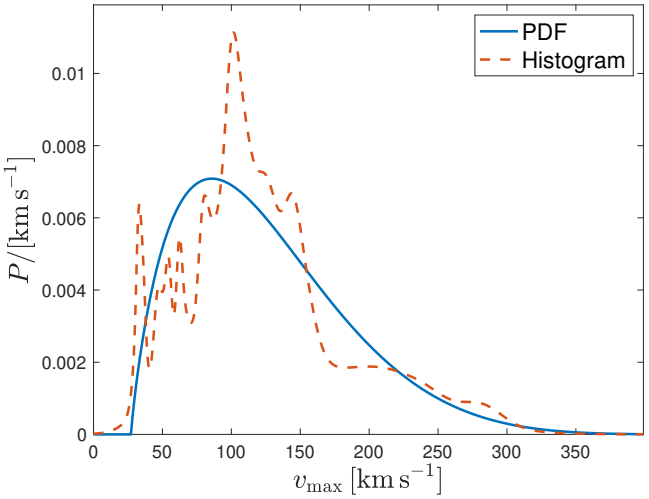

Figure 4. The distribution of the maximum rotational velocities ($v_{\rm max}$) for all 85 Sd galaxies (from Table 1, Column 10) with a mean $v_{\rm max}$ of $124.9 \pm 60.2\,{\rm km\,s^{-1}}$ and a median of $114.3 \pm 32.9\,{\rm km\,s^{-1}}$. The smoothed histogram (- - -) is generated from the summation of all 85 $v_{\rm max}$ measurements. The fitted PDF (——) peaks at $v_{\rm max} = 85.8 \pm 6.5\,{\rm km\,s^{-1}}$.

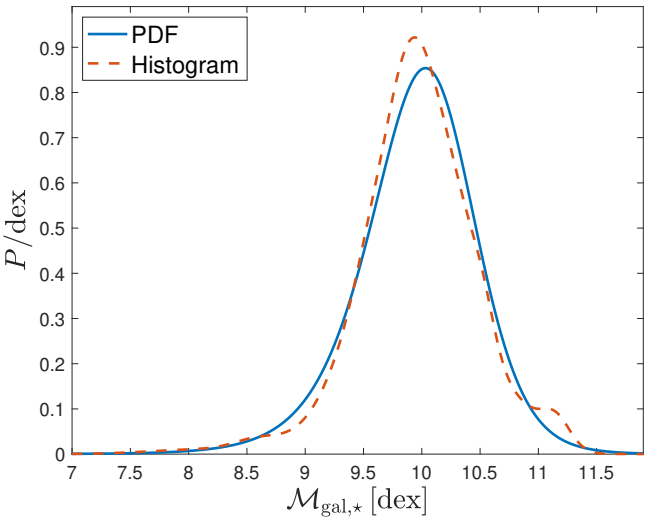

Figure 5. The distribution of the total galaxy stellar masses ($\mathcal{M}_{\rm gal,\star}$) for all 85 Sd galaxies (from Table 1, Column 8) with a mean $\mathcal{M}_{\rm gal,\star}$ of 9.96 ± 0.53 and a median of 9.97 ± 0.30. For comparison, Lacerda et al. (2020) found an average value of $\mathcal{M}_{\rm gal,\star} = 9.90 \pm 0.09$ from their sample of 34 Sd galaxies. The smoothed histogram (- - -) is generated from the summation of all 85 $\mathcal{M}_{\rm gal,\star}$ measurements. The fitted PDF (——) peaks at $\mathcal{M}_{\rm gal,\star} = 10.03 \pm 0.06$.

et al. 2001, 2003; Willott et al. 2007; Mortlock et al. 2011; Morganson et al. 2012; Kashikawa et al. 2015; Wu et al. 2015; Bañados et al. 2016, 2018; Decarli et al. 2018; Matsuoka et al. 2019; Onoue et al. 2019; Endsley et al. 2023). Furthermore, modeling of the quasar luminosity function suggests that the SMBH power sources of quasars were created from ancient *seeds* that were grown via accretion and mergers (*e.g.*, Soltan 1982; Small & Blandford 1992; Kauffmann & Haehnelt 2000; Volonteri & Rees 2005; Shankar et al. 2009; Shen et al. 2020; Lin et al. 2023; Li et al. 2023). Finding a possible mechanism for forming SMBHs in such a short time-scale is a primary concern and focus in modern astrophysics (see Haemmerlé et al. 2020; Inayoshi et al. 2020, for recent reviews). Not only observers, but theorist alike have tackled this problem, armed with N-body simulations and/or semi-analytic studies to discern the possible evolutionary scenarios that allow for the formation of massive seed black holes in high-redshift quasar host progenitors (Dijkstra et al. 2014; Visbal et al. 2014; Habouzit et al. 2016a,b; Lupi et al. 2021; Trinca et al. 2022; Bhowmick et al. 2022; Bennett et al. 2024; Jeon et al. 2023), with various success (see Di Matteo et al. 2023a, for a review).

The only proven pathway for the birth of black holes is from the death of massive stars, although exotic theories involving primordial black holes, inflation, and dark matter have been put forward (*e.g.*, Clesse & García-Bellido 2015; Chen et al. 2022; Davoudiasl et al. 2022; Hooper et al. 2023). It is unknown how the black hole remnants of even the most massive stars ($M_\bullet \approx 100\,{\rm M_\odot}$; *e.g.*, Fryer et al. 2001) could have grown to become SMBHs in the infancy of our Universe without extraordinary growth (Haiman & Loeb 2001). Studies of element abundance ratios and ionizing radiation from extremely metal-poor galaxies, combined with nucleosynthesis and photoionization models, indicate the past existence of supermassive ($>300\,{\rm M_\odot}$) stars (Kojima et al. 2021). These extinct stars (up to $10^3\,{\rm M_\odot}$) would have undergone core collapse, ejected roughly half their mass, and left behind $\gtrsim 100\,{\rm M_\odot}$ IMBHs remnants (Ohkubo et al. 2006). Nowadays, it is suspected that episodic periods of super-Eddington accretion (assuming there is an efficient way to channel gas towards the central black hole) is the natural solution to enable their rapid development (*e.g.*, Madau et al. 2014; Jiang et al. 2019;

Massonneau et al. 2023),[41] and coevolution of the massive progenitors with their host galaxies could even predate black hole formation (Bear & Soker 2020). In such scenarios, IMBHs would exist for fleeting moments of cosmic time and their detection would be unlikely.

Boco et al. (2020) predict that "heavy seeds" ($4 \lesssim \mathcal{M}_\bullet \lesssim 6$) could form in the star-forming progenitors of local early-type galaxies from the merging stellar compact remnants that have migrated, via gaseous dynamical friction, toward central high-density regions. Also, massive collapsing gas onto newborn protostars could create heavy seeds from several hundred to above $10^5\,M_\odot$ (Li et al. 2021). Alternatively, Tagawa et al. (2020) present a processes via stellar bombardment where supermassive protostars may grow to a range of masses as high as $\sim 10^5$–$10^6\,M_\odot$, and Schleicher et al. (2022) explain how massive metal-poor protoclusters could form IMBHs with $\mathcal{M}_\bullet \gtrsim 4$.[42] Additionally, "direct-collapse" models could spawn the genesis of heavy seeds (*e.g.*, Loeb & Rasio 1994; Bromm & Loeb 2003; Begelman et al. 2006; Lodato & Natarajan 2006; Hosokawa et al. 2013; Ferrara et al. 2014; Umeda et al. 2016; Haemmerlé et al. 2018a,b; Latif et al. 2020; Moriya et al. 2021). Such direct-collapse black hole scenarios would theoretically require overdense environments in the early Universe; observations of luminous quasars at cosmic density peaks are beginning to emerge (Overzier 2022).

In dense star clusters, either collisional runaway mergers of massive stars (Portegies Zwart & McMillan 2002; Davies et al. 2011; Lupi et al. 2014; Das et al. 2021; Rose et al. 2022; Vergara et al. 2023) or successive black hole mergers (Fragione et al. 2022a,b) could yield "intermediate-mass seeds" at a slightly lower range of masses ($3 \lesssim \mathcal{M}_\bullet \lesssim 4$). Moreover, dynamical interactions in young stellar clusters are dependent on initial mass and lead to distinct formation channels that can produce IMBHs (Di Carlo et al. 2021; Torniamenti et al. 2022). Despite their obscurity in observations, such IMBHs are not expected to be all that rare; modeling has shown that approximately one out of every 20 binary black hole mergers might involve IMBH seeds originating from stellar accretion and collisions in dense clusters (Arca Sedda et al. 2023b). Depending on the mass of IMBHs that are discovered, it will generate support or opposition for these various black hole seeding models. In particular, observational signatures and improved demography of IMBHs will help discriminate between the evolutionary pathways of light vs. heavy seeds and ascertain the nature of the first SMBH seeds (Greene 2012; Ricarte & Natarajan 2018; Sassano et al. 2021; Regan et al. 2023). The advancement of electromagnetic and gravitational radiation observatories over the coming decades should provide meaningful answers to these questions.

5.4.2. *Gravitational Radiation and Lenses*

The Laser Interferometer Gravitational-wave Observatory (LIGO; Abramovici et al. 1992; Abbott et al. 2009), with its "advanced" configuration (Harry & LIGO Scientific Collaboration 2010; LIGO Scientific Collaboration et al. 2015), may witness the formation of IMBHs through the early stages of runaway merger processes in dense NSCs (Fragione et al. 2020a,b; Fragione & Silk 2020; Escala 2021) and/or the merger of $\sim 10^2\,M_\odot$ black holes created from Population III stars (Fryer et al. 2001; Madau & Rees 2001; Haiman & Loeb 2001; Heger et al. 2003; Volonteri et al. 2003; Abadie et al. 2012; Abbott et al. 2017a; Kovetz et al. 2018; Antonini et al. 2019; Wang et al. 2022). Importantly, obtaining the merger rate density of binary IMBHs could constrain the initial mass function of Population III stars (Hijikawa et al. 2021). Initially in the first couple observing runs, no IMBH merger candidates were found (Abbott et al. 2017b; Abbott et al. 2019; Vajpeyi et al. 2022), but the past few years have yielded a couple IMBHs candidates with remnant masses of $156.3^{+36.8}_{-22.4}\,M_\odot$ (Abbott et al.

[41] Alternatively, Johnson & Upton Sanderbeck (2022) show that sustained super-Eddington accretion can overcome early, inefficient radiation and proceed unabated until the initial gas supply is exhausted. Also, Sassano et al. (2023) point out that episodic super-Eddington accretion onto medium-weight seeds ($M_\bullet \sim 10^3\,M_\odot$) rapidly quenches by supernova feedback after $\sim$1 Myr, and therefore is only able to grow to $M_\bullet \lesssim 10^6\,M_\odot$. Additionally, strong primordial seed magnetic fields can increase the mass growth rate of supermassive stars (Hirano et al. 2021) and moderate Lyman-Werner ultraviolet backgrounds can allow for the production of massive Population III stars (Latif et al. 2021) that later collapse to IMBHs (Spera & Mapelli 2017; Renzo et al. 2020; Costa et al. 2023). Shi et al. (2023) envision the possibility of hyper-Eddington growth in dense clouds that are able to rapidly form IMBHs from the runaway growth of stellar-mass seeds. "Super-competitive accretion" (*e.g.*, Schleicher et al. 2023) is another proposed mechanism for the formation of very massive objects in the early Universe. In an extreme scenario, Haemmerlé et al. (2021) investigate the maximum accretion rate of supermassive stars and find that such stars could potentially accrete to $>10^6\,M_\odot$ before collapse, thus directly birthing SMBHs.

[42] The JWST may have discovered evidence for a proto-globular cluster hosting a supermassive star at $z = 10.6$ (Charbonnel et al. 2023).

2021)[43] and *possibly* $172.9^{+37.7}_{-33.6}\,M_\odot$ (The LIGO Scientific Collaboration et al. 2021, *cf.* Abbott et al. 2022).

The proposed third-generation ground-based gravitational-wave observatory, the Cosmic Explorer, will be able to observe $100\,M_\odot$–$100\,M_\odot$ merging black holes at $z > 10$ (Evans et al. 2021). The planned Laser Interferometer Space Antenna (LISA; Amaro-Seoane et al. 2017, 2023) will be more sensitive to longer wavelength (*i.e.*, lower frequency) gravitational waves (Einstein 1916) than the LIGO, emanating from sources such as the inspiral of binary IMBHs (*e.g.*, Li 2004; Portegies Zwart et al. 2004; Will 2004; Chen 2020) and extreme-mass ratio inspirals (EMRIs) involving compact stellar-mass objects such as black holes, white dwarfs, and neutron stars swirling around and merging with IMBHs and SMBHs (*e.g.*, Gair 2009; Holley-Bockelmann et al. 2010; Mapelli et al. 2012a; Amaro-Seoane et al. 2013) or even in the interiors of supermassive stars (Raveh et al. 2021), including an important contribution of primary sources from IMBH–SMBH binaries (Fragione 2022). Particularly, modeling by Izquierdo-Villalba et al. (2023) shows that the LISA will detect coalescing massive black hole binaries with total masses of 10^4–$10^5\,M_\odot$ in host galaxies that are predominantly "extreme late-types" (*i.e.*, akin to our Sd galaxies) at $z = 1.5$–3.0.[44] A more complete picture of low-frequency gravitational waves will be possible via joint detections between LISA and TianQin (Torres-Orjuela et al. 2023). Successive space-based detectors will be able to fill in the gaps in the gravitational-wave spectrum: μHz detectors will observe intermediate-mass ratio inspirals (IMRIs) involving IMBHs inspiraling onto SMBHs (Sesana et al. 2021) and dHz detectors will be "perfectly suited" to study IMBHs in the range $\sim 10^2\,M_\odot$–$10^4\,M_\odot$ (Arca Sedda et al. 2020). The prospective Atom Interferometer Observatory and Network (AION; Badurina et al. 2020, 2022) will excel at measuring the ringdown stages and high-frequency tails of merging IMBH binaries. Together, the combined multi-band synergy of space- and ground-based gravitational-wave detectors will be able to broadly explore the population of IMBHs at cosmological distances (Jani et al. 2020; Fragione & Loeb 2023).

The number densities obtained from such EMRIs (and complementary electromagnetic observations, *e.g.*, Blecha et al. 2006; Clausen & Eracleous 2011; Andreoni et al. 2017) should prove vital to constraining the BHMF at low-masses out to $z \approx 1$ (Gair et al. 2010). The LISA combined with joint observations made by future wide-survey telescopes will greatly advance multi-messenger localization of black hole merging events in the low-redshift Universe (Saini et al. 2022; Piro et al. 2023b; Bardati et al. 2023), but at high-redshifts, the localization of electromagnetic counterparts will be challenging (Chakraborty et al. 2023; Dong-Páez et al. 2023a). The prospect of reliably observing electromagnetic counterparts that accompany the LISA detections of high-z lower-mass black holes remains pessimistic (Pacucci et al. 2017; Dong-Páez et al. 2023b); Mangiagli et al. (2022) estimate that as few as one electromagnetic counterpart will be observed for every two years that the LISA operates. Indeed, Volonteri et al. (2023) find that only relatively over-massive black holes, indicative of heavy seeds, would be observable by the *James Webb* Space Telescope (JWST; Gardner et al. 2006) at $z > 9$. As an added bonus, gravitational-wave cosmology with EMRIs will provide tight constraints on the Hubble constant, H_0 (Laghi et al. 2021). Furthermore, the LISA is expected to greatly aid in reconstructing the contribution that mergers have made in the formation of massive black holes—remarkably, even in protogalaxies at high-z beyond the reach of conventional telescopes (Sesana et al. 2011)—as compared with the plasma-fed growth of massive black holes (*e.g.*, Soltan 1982; Shankar et al. 2004). Before then, a greater knowledge of the local BHMF, including the abundance of IMBHs, will be helpful for establishing the optimal mission capabilities and lifetimes required to detect sufficient gravitational-wave signals from as many astrophysical phenomena as possible (see Arca Sedda et al. 2023c, for a review of gravitational-wave sources in galactic nuclei).

Because of its unique ability to reveal the presence of isolated compact objects that emit little or no light, microlensing has long been recognized as an important tool to find black holes (Agol et al. 2002). Sure enough, "the first unambiguous detection and mass measurement of an isolated stellar-mass black hole" was recently found in our Galaxy via microlensing (Lam et al. 2022; Sahu

[43] This gravitational-wave event (GW190521) is further speculated to be the result of the merger of central black holes from two ultradwarf galaxies (Palmese & Conselice 2021). Furthermore, GW190521 poses important implications for the lower boundary of the so-called "pair-instability mass gap" (O'Brien et al. 2021). Anagnostou et al. (2022) propose that the mass gap was bridged by multiple mergers in the core of a globular cluster. Alternatively, other proposed scenarios liken GW190521 to be the result of an intermediate-mass ratio inspiral involving an IMBH, and thus consisted of an IMBH both before and (slightly larger) after the merger, avoiding the pair-instability mass gap (Fishbach & Holz 2020; Nitz & Capano 2021). The GW190521 event is also perceived to have taken place inside an AGN (Morton et al. 2023).

[44] For this endeavor, the *Roman* Space Telescope will be able to aid in finding precursors, *i.e.*, massive black hole binaries before their separations are quite small enough to be detected via gravitational waves with the LISA (Haiman et al. 2023).

et al. 2022a). Furthermore, concerted study of globular clusters in our Galactic neighborhood over a baseline of a couple decades has a high probability of detecting the presence of any IMBHs that might reside in the clusters (Kains et al. 2016). In particular, Anagnostou et al. (2022) estimate that ≈1%–10% of median-mass globular clusters will produce an IMBH through hierarchical mergers, in the absence of gravitational-merger recoil.[45] Indeed, potential IMBHs housed in globular clusters have been piling up in the literature (Noyola et al. 2008; Lin et al. 2020a; Vitral et al. 2023); such as in the Galactic globular cluster 47 Tucanae (Kızıltan et al. 2017).[46] Because globular clusters are suspected to nurse IMBHs, globular clusters orbiting close to the Galactic Center could serve as important delivery vehicles of IMBHs into the innermost regions of the Milky Way, while also emitting low-frequency gravitational waves (Arca Sedda et al. 2019; Leveque et al. 2023). Indeed, there is evidence of IMBH candidates around our Galactic Center (*e.g.*, Oka et al. 2017) that may be further constrained by the LISA (Strokov et al. 2023), but the purported IMBHs may not have been born near the Milky Way's center (Ballone et al. 2018, 2021).

Emerging evidence indicates that the true population is significant and that the Universe might be rife with IMBHs. Recently, Paynter et al. (2021) presented a novel way to search for and find IMBHs as the intervening gravitational lenses to distant gamma ray bursts (GRBs). They claim to have discovered an IMBH at $z \approx 1$, which is lensing a background GRB at $z \approx 2$. Depending on the unknown redshift, they estimate the mass of the lensing object to be $\approx 5.5 \times 10^4\,M_\odot$, which they interpret as evidence for an IMBH. Based upon the observed frequency of lensed GRBs, they estimate that the present-day number density of IMBHs with masses between $\approx 10^4$–$10^5\,M_\odot$ is $\approx 2.3 \times 10^3\,\mathrm{Mpc}^{-3}$. Compared with our aforementioned estimate of $> 4.96 \times 10^{-6}\,\mathrm{Mpc}^{-3}$ for central IMBHs, this implies that the *vast* majority of IMBHs are not in the center of galaxies.

5.4.3. *Star Clusters*

Young, globular, and NSCs all distinctly contribute to the hierarchical mergers of black holes, as evidenced by the unique mass and rate of mergers they produce (Mapelli et al. 2021a,b). NSCs serve as important waypoints in the hierarchical buildup of SMBHs (see Neumayer et al. 2020, for a review of NSCs). Young dense massive star clusters can rapidly produce IMBHs on time-scales $\lesssim 15\,\mathrm{Myr}$ (Rizzuto et al. 2021) and involve a range of black hole merger events that nearly cover the complete mass range for current ground-based gravitational-wave detections (Rizzuto et al. 2022). A new theory of so-called "Feedback-Free Starbursts" that allows for efficient star formation and massive galaxies at cosmic dawn may help explain the formation of IMBH seeds in rapidly-constructed star clusters (Dekel et al. 2023). Furthermore, gas-rich NSCs can act as a long-lived channel that continuously forms IMBHs throughout cosmic time, not just at high-z (Natarajan 2021).

Simulations show that nucleated dwarf galaxies are prime environments for extremely efficient mergers of IMBHs (Khan & Holley-Bockelmann 2021). Tidal stripping of nucleated dwarf galaxies yield ultracompact dwarf galaxies (*e.g.*, Ferrarese et al. 2016; Graham 2020; Pechetti et al. 2022; Dumont et al. 2022), which can ultimately become the captured nuclei of previously bulgeless galaxies via mergers, with their IMBHs in tow (Graham et al. 2021a). X-ray activity in the centers of low-mass galaxies, like those in our sample, can indicate the presence of nuclear IMBHs (Graham et al. 2019, 2021b). At the end of their evolutionary fates, massive NSCs (built from ultracompact dwarf galaxies and/or massive globular clusters) composed of clusters of IMBHs can build an SMBH before partial dispersion of the cluster, releasing copious energy via gravitational waves in the process (Chassonnery & Capuzzo-Dolcetta 2021). Mayes et al. (2023) compare observations of ultracompact dwarf galaxies and simulated stripped nuclei, finding similar numbers of SMBHs in each, and specifically that ≈50% of stripped nuclei more massive than $2 \times 10^6\,M_\odot$ should contain SMBHs.

Today, most galactic nuclei are known to harbor SMBHs, and a significant fraction of those SMBHs are found to coexist with NSCs.[47] Similarly, most massive galaxies possess NSCs (Ashok et al. 2023), however, not all nucleated galaxies possess SMBHs. Askar et al. (2021, 2022) investigated the delivering, retention, and growth of seed IMBHs in NSCs. Their work

[45] Asymmetric gravitation-wave emission during mergers can eject remnants from clusters at high velocities, thus hindering further growth via black hole mergers with a cluster. However, stellar interactions with an IMBH can similarly fling stars out of cluster; the rates and velocities of stellar ejections can help indicate the presence and mass of IMBHs responsible for the ejected stars (see Weatherford et al. 2023, and references therein).

[46] However, the validity of such attestations are still debated (Strader et al. 2012; Tremou et al. 2018; Hénault-Brunet et al. 2020; Dickson et al. 2023).

[47] For galaxies that possess both an SMBH and an NSC, Sruthi & Ravikumar (2023) found an interesting demarcation between red and blue galaxies, such that red galaxies possess SMBHs that are more massive than their NSCs and *vice versa* for blue galaxies.

highlights the $M_{\rm gal,\star}$-dependent occupation fraction of SMBHs in NSCs, based on the growth of seed IMBHs via gravitational-wave mergers and gas accretion. Particularly, gravitational-wave recoil kicks can lead to the ejection of seed IMBHs, and thus unrealized SMBHs in some NSCs, preferentially in lower-mass galaxies with lower-mass NSCs and lower escape velocities (Amaro-Seoane & Freitag 2006; Gürkan et al. 2006; Amaro-Seoane et al. 2007; Arca Sedda & Mastrobuono-Battisti 2019; Arca Sedda et al. 2023a) or if the mass ratio $q \gtrsim 0.15$ (Askar et al. 2021).[48] However, more massive NSCs (with escape velocities $\gtrsim$400 km s^{-1}) inevitably form high-mass IMBHs (Chattopadhyay et al. 2023). Furthermore, Kroupa et al. (2020) found that an SMBH can only form in a spheroid with mass $\gtrsim 10^{9.6}$ M$_\odot$, otherwise, only an accumulated NSC remains. Following on, Mahani et al. (2021) further described how ultra-compact dwarf galaxies might not possess IMBHs, but rather only compact sub-clusters of normal black holes and neutron stars that might resemble an IMBH when viewed at low resolution.

5.4.4. *Tidal Disruption Events*

Usually, observations are biased towards detecting the most massive SMBHs. However, some physical processes, like TDEs, are only produced by less massive black holes (Hills 1975; Rees 1988). Particularly, if an SMBH's event horizon is larger than the tidal radius of the SMBH–star system, the in-falling star will be swallowed whole and not produce a TDE, which effectively rules out TDEs from $\gtrsim 10^8$ M$_\odot$ (*cf.* $\gtrsim 10^7$ M$_\odot$, as pointed out by Coughlin & Nixon 2022; Nicholl et al. 2022, owing to a population of tidally-destroyed stars that is dominated by low-mass stars) black holes (MacLeod et al. 2012). For TDEs involving IMBHs, encounters with main-sequence stars will lead to successive close passages where the IMBH will repeatedly nibble away at the star and ultimately eject the stellar remnant. Kıroğlu et al. (2023) simulated such TDEs and found that the number of electromagnetic flares from repeated close passages decreases with increasing mass of the black hole, thus establishing a methodology to determine the mass and identify IMBHs via the number of observed flares.

Whereas observations to-date have witnessed the disruption of non-degenerate stars, another subcategory of TDE involving IMBHs and white dwarfs are expected to exist (*e.g.*, Luminet & Pichon 1989; Rosswog et al. 2009; Clausen & Eracleous 2011; Haas et al. 2012; Cheng & Bogdanović 2014; MacLeod et al. 2016; Vick et al. 2017; Tanikawa et al. 2017; Tanikawa 2018; Maguire et al. 2020; Chen et al. 2023b; Lam et al. 2022). For this subclass of tidally-induced thermonuclear transient (Ia-TDE; similar to, but less luminous than a Type Ia supernova), the mass of the black hole must be $\lesssim 10^5$ M$_\odot$ (Kobayashi et al. 2004; Rosswog et al. 2009; Gezari 2021). As such, systematic searches for Ia-TDE candidates in time-domain surveys will look for confirmation of Ia-TDEs and thus, unambiguous evidence of *bona fide* IMBHs (Velazquez & Gezari 2022; Gomez & Gezari 2023). This presents an opportunity to exclusively identify lower-mass black holes and extend black hole mass scaling relations down to lower masses (*e.g.*, Ramsden et al. 2022). In addition to electromagnetic, gravitational radiation would be detectable during the inspiral of a tidal stripping event. Specifically, Chen et al. (2023b) estimated that the space-borne gravitational-wave detectors will be able to witness the tidal stripping of white dwarfs by IMBHs within the Local Supercluster ($\sim$33 Mpc).

Combining our previous topics of discussion, black hole seeding and NSCs, can help to explain the rapid growth of massive black holes in galactic nuclei. Lee et al. (2023) explore how black hole seeds may grow expeditiously via both gas accretion and tidal disruption accretion in dense NSCs. Stone et al. (2017) presented (and Baldassare et al. 2022 provided observational support for) a scenario, whereby NSCs can transform into SMBHs via runaway tidal encounters when $\sigma_0 \gtrsim 40$ km s^{-1} for a cluster. Thus, the rate of observed TDEs can help divulge black hole seeding mechanisms, as well as the BHMF (Stone & Metzger 2016; Yao et al. 2023; Coughlin & Nicholl 2023).

Recent observations of TDEs involving IMBHs (Perley et al. 2019; Lin et al. 2020b; Wen et al. 2021; Angus et al. 2022) are helping to establish their frequency, and samples of TDEs (particularly in dwarf galaxies) are beginning to grow (Molina et al. 2021). Particularly of interest, Pfister et al. (2020) showed the TDE rate is enhanced by up to two orders of magnitude in nucleated galaxies over the observed rate in non-nucleated galaxies. However, it is important to disambiguate between complete *total* (*i.e.*, total stellar destruction) and *partial* (*i.e.*, a stellar remnant survives) TDEs (the latter of which is particularly relevant for nucleated galaxies) to reconcile theoretical and observed rates (Bortolas et al. 2023). Finally, while TDEs are typically detected in wide-field optical and X-ray surveys, it is important to also utilize infrared surveys to look for dust-obscured TDEs in star-forming galaxies (Panagiotou et al. 2023).

[48] Akiba & Madigan (2021, 2023) show how unique signatures are left in NSCs after gravitational-wave recoil kicks, which can inform observational searches for recoiling massive black holes.

5.4.5. *Dwarf Galaxies and Evolution*

As more and more studies are examining the population of black holes in dwarf galaxies, the evidence is growing that these tiny galaxies are a linchpin in hierarchical galaxy evolution. Indeed, Rashkov & Madau (2014) expect that many IMBHs have been left to wander the halo of our Milky Way as relics of hierarchical merging of progenitor dwarf galaxies.[49] The last decade of research has reversed the traditional view that massive black holes are only found in the nuclei of giant galaxies (see Reines 2022, for a review). In fact, Greene et al. (2020) estimated that the occupation fraction of black holes with $10^4\,M_\odot \lesssim M_\bullet \lesssim 10^6\,M_\odot$ residing in galaxies with $10^9\,M_\odot \lessapprox M_{\rm gal,\star} \lessapprox 10^{10}\,M_\odot$ is $\gtrsim$50%. Although numerous observational searches for IMBHs in dwarf galaxies have increasingly yielded more candidate detections (*e.g.*, Dong et al. 2007; Farrell et al. 2009; Reines et al. 2013; Lin et al. 2016; Ferré-Mateu et al. 2021; Mićić et al. 2022; Salehirad et al. 2022; Hatano et al. 2023a,b), difficulties still abound in attempts to reproduce the results in simulations (Haidar et al. 2022). Furthermore, feedback from central black holes in massive galaxies is known to substantially affect their mutual evolution, but stark disagreement persists between simulations (Lanfranchi et al. 2021) and observations (Davis et al. 2022). Additionally, a growing population of dwarf galaxies have been observed to possess low-luminosity AGNs along with some evidence of jets and outflow activity, likely resulting from accreting IMBHs (Mezcua et al. 2016, 2018; Mezcua & Domínguez Sánchez 2020; Schutte & Reines 2022; Yang et al. 2023).

With improved knowledge of black holes in dwarf galaxies, resolving the BHMF at $M_\bullet < 10^5\,M_\odot$ will be a critical test for black hole formation/feedback models and should help clarify if black hole mass scaling relations might differ, as determined by their seeding mechanisms (Volonteri et al. 2008; van Wassenhove et al. 2010; Zaw et al. 2020; Silk 2017; Barai & de Gouveia Dal Pino 2019; Goradzhanov et al. 2022). In their study of the (stellar mass)–(halo mass) relation for Local Group dwarf galaxies, Zaritsky & Behroozi (2023) found that some galaxies require additional interior mass beyond what the standard dark matter profile predicts, which they speculate is accounted for by central IMBHs that encompass a relatively large (one to a few) percent of the halo masses. Moreover, there is mounting evidence that the slope of the $M_\bullet$–$M_{\rm gal,\star}$ relation might be flatter in the dwarf-mass regime than in the high-mass regime (Spinoso et al. 2023), *i.e.*, the dwarf (and low-stellar mass) galaxies' black holes can be over-massive with respect to the extrapolated relation from higher masses (Reines et al. 2011; Secrest et al. 2017; Mezcua et al. 2023; Weller et al. 2023a; Stone et al. 2023a; Maiolino et al. 2023a; Pacucci et al. 2023a). Particularly, Sanchez et al. (2023) demonstrated from simulations that black holes at the low-mass end of the $M_\bullet$–σ_0 relation appear over-massive due to their feedback efficiency, causing mass redistribution by expelling gas and metals from the inner regions of their host galaxies.[50] In addition, increased insights into the IMBH occupation fraction will be of benefit to black hole seeding theories (Chadayammuri et al. 2023); simulations reveal that the black hole occupation fraction is highly-dependent on the black hole seeding efficiency (Spinoso et al. 2023). This will also allow for extension of black hole mass scaling relations to a lower regime (*e.g.*, Graham & Scott 2013; Graham 2023b,c; Graham & Sahu 2023a,b; Savorgnan et al. 2013, 2016; Savorgnan 2016a,b; Davis et al. 2017, 2018, 2019a,b,c, 2021; Davis & Jin 2023; Sahu et al. 2019a,b, 2020, 2022b,c; Sahu 2021, 2022; Jin & Davis 2023), which should undoubtably provide valuable insights into the evolution of black holes. Improved knowledge of the coevolution of black holes and their host galaxies (via macroscopic galactic properties) will better facilitate calculations of the black hole mass density in the Universe (*e.g.*, Graham et al. 2007; Davis et al. 2014; Mutlu-Pakdil et al. 2016), as well as elucidating the evolutionary history of black holes.

5.4.6. *Future Work and Possible Observations*

In their investigation of the accretion disks around IMBHs, Ogata et al. (2021) predicted that IMBHs could be observed as bright sources in the infrared band. Furthermore, Cann et al. (2018, 2021) have shown that infrared coronal lines can find AGNs even when optical diagnostics fail, as demonstrated in their study of an optically-normal, low-metallicity dwarf galaxy. As such, coronal lines are ideal and the infrared JWST will be well-suited for spotting IMBHs (Reefe et al. 2022, 2023, *cf.* Herenz et al. 2023). Armed with superior sensitivity, resolution, and spectroscopic multiplexing capabilities, the ongoing JWST observations will provide a boon to scientific discovery (Kalirai 2018).

Impressively, the JWST has quickly found confirmed galaxies up to $z = 13.2$ (Curtis-Lake et al. 2023) and

[49] See the Pacucci et al. (2023b) white paper, which explores the detectability of IMBHs wandering our Galaxy.

[50] However, we note that there is not a consensus on the behavior of the low-mass end of the $M_\bullet$–σ_0 relation. For instance, Pacucci et al. (2018) contrarily anticipate that low-mass galaxies host under-massive central black holes.

candidate objects up to an incredible $z \approx 20$ (Yan et al. 2023),[51] as well as surprisingly massive galaxies (up to $\sim 10^{11}\,M_\odot$) at $7.4 < z < 9.1$ (Labbé et al. 2023). Already testing the onset of spiral galaxy formation, the JWST has helped identify a dusty multiarm spiral galaxy at $z = 3.06$ (Wu et al. 2023) and found that disk galaxies are prevalent out to at least $z = 9.5$ (Kartaltepe et al. 2023; Sun et al. 2023b) Similarly, the JWST has enabled the identification of the most distant barred galaxies to-date, out to $z \simeq 3$ (Guo et al. 2023; Huang et al. 2023; Costantin et al. 2023). Of particular interest to black hole seeding and early BH–galaxy assembly, the JWST has discovered a crop of low-mass (under-massive; Stone et al. 2023b) galaxies at high redshifts (Kocevski et al. 2023; Looser et al. 2023b; Gelli et al. 2023; Strait et al. 2023; Curtis-Lake et al. 2023; Robertson et al. 2023; Williams et al. 2023a; Übler et al. 2023).

The JWST has the ability to color-select black hole seeds transitioning to SMBHs (Goulding & Greene 2022) and distinguish rest-frame optical lines for the identification of "light seed" Population III (Vanzella et al. 2023) and "heavy seed" direct-collapse black holes in the early Universe (Nakajima & Maiolino 2022). Models estimate that the JWST surveys will have the sensitivity to detect heavy black hole seeds out to redshifts of $z \lesssim 14$ (Trinca et al. 2023). Already, the JWST has spotted high-redshift AGNs (Larson et al. 2023; Maiolino et al. 2023b,a) and established constraints on their formation that requires either super-Eddington accretion from a stellar mass seed or Eddington accretion from a very massive black hole seed. Moreover, the JWST has already witnessed an X-ray quasar ($M_\bullet \sim 4 \times 10^7\,M_\odot$ in a comparably massive host galaxy) at $z = 10.3$, which "suggests that early SMBHs originate from heavy seeds" (Bogdán et al. 2023; Natarajan et al. 2023; Goulding et al. 2023) and constitutes the first outsize (née obese) black hole galaxy (Natarajan et al. 2017). Radio observations from the forthcoming Square Kilometre Array could also detect emissions from direct-collapse black holes at high-z (Whalen et al. 2020, 2023). The parameters for black hole growth and seed models will become significantly constrained as future observations discern $z > 8$ quasars (Pacucci & Loeb 2022).

In order to dynamically confirm the IMBH mass estimates we have made, it would be necessary to resolve kinematics within the gravitational sphere of influence (SOI) of our black holes. From Peebles (1972),[52] a black hole at the center of a galaxy has an SOI with a radius $r_h \equiv GM_\bullet\sigma_0^{-2}$. From our sample of 23 targets of interest, UGC 3949 is the only galaxy with a known central velocity dispersion ($\sigma_0 = 70.1 \pm 4.9\,\mathrm{km\,s^{-1}}$). For UGC 3949 ($d = 89.9 \pm 6.9$ Mpc and $M_\bullet = 5.05 \pm 2.99 \times 10^4\,M_\odot$), we obtain $r_h = 44.2 \pm 26.8$ mpc $= 101 \pm 62\,\mu$as.

With its stunning resolution of 20 μas, the Event Horizon Telescope (EHT) could resolve this region in the center of UGC 3949. The EHT resolved the emission rings surrounding the SMBHs M87* and Sgr A* with diameters of $\approx$42 μas (Event Horizon Telescope Collaboration et al. 2019; Medeiros et al. 2023) and $\approx$52 μas (Event Horizon Telescope Collaboration et al. 2022), respectively. Indeed, distance alone would not be a hinderance in resolving similarly-sized IMBHs in our sample of targets, which only extends out to about 125 Mpc. Granted, even if the SOI were resolved in images of our targets, spectra would still be useful.

We hope to target the 23 candidates with follow-up spectroscopy (for stellar velocity dispersions, gas emission lines, and black hole virial mass estimates[53]), X-ray imaging (for AGNs activity), and perhaps simultaneous radio interferometry (for the fundamental plane of black hole activity; Merloni et al. 2003; Falcke et al. 2004).[54] Further X-ray information such as the characteristic variability or the normalized excess variance (variability amplitude) can also be used to estimate black hole masses of AGNs (Pan et al. 2015). However, the characteristic damping timescale at X-ray wavelengths is substantially shorter (González-Martín & Vaughan 2012), and less correlated with black hole mass, than at optical wavelengths (Burke et al. 2021).[55] Additionally, the variability timescale at sub-millimeter wavelengths

[51] Qin et al. (2023) found that boosted star-formation efficiencies and reduced feedback regulation are necessary to reproduce $z \gtrsim 16$ JWST galaxy candidates, which are susceptible to low-redshift contamination from $z \sim 5$ galaxies. See also the cautionary report from Zavala et al. (2023) that detailed how dusty starbursts at lower redshifts can masquerade as ultra-high photometric redshift galaxies in JWST observations. Furthermore, it is worth investigating the implications of bursty star formation at high redshifts leading to selection effects and associated biases for the JWST (Sun et al. 2023a; Looser et al. 2023a).

[52] See also the corresponding §3.3 from Davis & Graham (2021).

[53] Cho et al. (2023) elucidate how better constraints for the Hα size–luminosity relation are required to calibrate a virial mass estimator based on the Hα broad emission line from low-luminosity AGNs and IMBHs.

[54] However, Gültekin et al. (2022) cautioned against the use of the fundamental plane of black hole activity for identifying IMBHs without additional constraints beyond just straightforward X-ray and radio observations. Furthermore, only a small fraction ($\sim$0.6%) of IMBH candidate host galaxies are radio-band active (Yang & Yang 2023).

[55] Although, Treiber et al. (2023) revealed the substantial effect of contamination from variable stars in their search for stochastic variability.

appears to also be a useful parameter that correlates well with black hole mass in low-luminosity AGNs (Chen et al. 2023a).

5.5. *Concluding Remarks*

The comparisons throughout this work seem to indicate that Sd galaxies exhibit characteristics that are surprisingly similar to the general population of spiral galaxies, in the aggregate, although we did not explore bulge mass, as many Sd galaxies are (considered) bulgeless. However, we note that a range of B/T flux ratios exist at each morphological type (Graham & Worley 2008). This unexpected resemblance could be a symptom of subjective morphological misclassifications, or perhaps is showing a natural diversity even amongst this subpopulation of apparent late-type spiral galaxies. Specifically, we find the expectation that an archetypical Sd should have a low mass, be slowly rotating, display loosely wound spiral arms, and have a low-mass central hole is not unimpeachable; characteristics more akin to earlier type spiral galaxies appear to be endemic. Thus, the classical Sd morphological class is a stereotype; there is no average Sd galaxy. In any regard, we do find merit in exploring Sd galaxies for IMBHs, as they possess the requisite environmental traits (for hosting IMBHs) in a higher proportion than the average spiral galaxy.

On the whole, we find that a randomly selected Sd galaxy will have a 27.7% chance of possessing an IMBH. Our search has produced 23 candidates, each with a probability of at least 50% of hosting an IMBH. Although we expect 23/85 of our galaxies house an IMBH, the product of all their $P(\mathcal{M}_\bullet \leq 5)$ probabilities implies an ≈100% certainty that at least one of our 85 Sd galaxies possess an IMBH. We intend to make these targets the focus of continued research. The fruition of the long-sought quest to identify IMBHs will finally complete the gap in our knowledge of the demography of black holes.

BLD thanks David Nelson for the use of his secluded office space during the COVID-19 pandemic. The Australian Research Council's funding scheme DP17012923 supported this research. Parts of this research were conducted by the Australian Research Council Centre of Excellence for Gravitational-wave Discovery (OzGrav), through project number CE170100004. This material is based upon work supported by Tamkeen under the NYU Abu Dhabi Research Institute grant CASS. This research has made use of NASA's Astrophysics Data System, and the NASA/IPAC Extragalactic Database (NED) and Infrared Science Archive (IRSA). We acknowledge use of the HyperLeda database (http://leda.univ-lyon1.fr) and the Reference Catalog of galaxy SEDs (http://rcsed.sai.msu.ru/).

Facilities: CXO, GALEX, Pan-STARRS1, & SDSS.

Software:

`2DFFT` (Davis et al. 2016)
`2DFFT Utilities`
`2DFFTUtils Module`
`Astropy` (Astropy Collaboration et al. 2013, 2018)
`Hyper-Fit` (Robotham & Obreschkow 2015, 2016)
`IRAF` (Tody 1986, 1993)
K`-corrections calculator`
`Matplotlib` (Hunter 2007)
`NumPy` (Harris et al. 2020)
`Pandas` (McKinney 2010)
`pearspdf`
`PySR` (Cranmer 2023)
`Python` (Van Rossum & Drake 2009)
`SAOImageDS9` (Joye & Mandel 2003)
`SciPy` (Virtanen et al. 2020)
`SpArcFiRe` (Davis & Hayes 2014)
`Spirality` (Shields et al. 2015)
`uncertainties`

ORCID IDS

Benjamin L. Davis
https://orcid.org/0000-0002-4306-5950
Alister W. Graham
https://orcid.org/0000-0002-6496-9414
Roberto Soria
https://orcid.org/0000-0002-4622-796X
Zehao Jin (金泽灏)
https://orcid.org/0009-0000-2506-6645
Igor D. Karachentsev
https://orcid.org/0000-0003-0307-4366
Elena D'Onghia
https://orcid.org/0000-0003-2676-8344

REFERENCES

Abadie, J., Abbott, B. P., Abbott, R., et al. 2012, PhRvD, 85, 102004

Abbott, B. P., Abbott, R., Adhikari, R., et al. 2009, Reports on Progress in Physics, 72, 076901

Abbott, B. P., Abbott, R., Abbott, T. D., et al. 2016, PhRvL, 116, 061102

—. 2017a, PhRvD, 96, 022001

—. 2017b, PhRvD, 96, 022001

Abbott, B. P., Abbott, R., Abbott, T. D., et al. 2019, Phys. Rev. X, 9, 031040

Abbott, R., Abbott, T. D., Abraham, S., et al. 2021, Physical Review X, 11, 021053

Abbott, R., Abbott, T. D., Acernese, F., et al. 2022, A&A, 659, A84

Abdeen, S., Kennefick, D., Kennefick, J., et al. 2020, MNRAS, 496, 1610

Abdeen, S., Davis, B. L., Eufrasio, R., et al. 2022, MNRAS, 512, 366

Abramovici, A., Althouse, W. E., Drever, R. W. P., et al. 1992, Science, 256, 325

Agol, E., Kamionkowski, M., Koopmans, L. V. E., & Blandford, R. D. 2002, ApJL, 576, L131

Akiba, T., & Madigan, A.-M. 2021, ApJL, 921, L12

—. 2023, arXiv e-prints, arXiv:2305.03054

Aktar, R., Xue, L., Zhang, L.-X., & Luo, J.-Y. 2023, arXiv e-prints, arXiv:2309.17271

Amaro-Seoane, P., & Freitag, M. 2006, ApJL, 653, L53

Amaro-Seoane, P., Gair, J. R., Freitag, M., et al. 2007, Classical and Quantum Gravity, 24, R113

Amaro-Seoane, P., Sopuerta, C. F., & Freitag, M. D. 2013, MNRAS, 429, 3155

Amaro-Seoane, P., Audley, H., Babak, S., et al. 2017, arXiv e-prints, arXiv:1702.00786

Amaro-Seoane, P., Andrews, J., Arca Sedda, M., et al. 2023, Living Reviews in Relativity, 26, 2

Anagnostou, O., Trenti, M., & Melatos, A. 2022, ApJ, 941, 4

Andreoni, I., Ackley, K., Cooke, J., et al. 2017, PASA, 34, e069

Angus, C. R., Baldassare, V. F., Mockler, B., et al. 2022, Nature Astronomy, 6, 1452

Antonini, F., Gieles, M., & Gualandris, A. 2019, MNRAS, 486, 5008

Arca Sedda, M., Askar, A., & Giersz, M. 2019, arXiv e-prints, arXiv:1905.00902

Arca Sedda, M., Kamlah, A. W. H., Spurzem, R., et al. 2023a, MNRAS, 526, 429

Arca Sedda, M., Mapelli, M., Benacquista, M., & Spera, M. 2023b, MNRAS, 520, 5259

Arca Sedda, M., & Mastrobuono-Battisti, A. 2019, arXiv e-prints, arXiv:1906.05864

Arca Sedda, M., Naoz, S., & Kocsis, B. 2023c, Universe, 9, 138

Arca Sedda, M., Berry, C. P. L., Jani, K., et al. 2020, Classical and Quantum Gravity, 37, 215011

Ashok, A., Seth, A., Erwin, P., et al. 2023, arXiv e-prints, arXiv:2308.03913

Askar, A., Davies, M. B., & Church, R. P. 2021, MNRAS, 502, 2682

—. 2022, MNRAS, 511, 2631

Astropy Collaboration, Robitaille, T. P., Tollerud, E. J., et al. 2013, A&A, 558, A33

Astropy Collaboration, Price-Whelan, A. M., Sipőcz, B. M., et al. 2018, AJ, 156, 123

Bañados, E., Venemans, B. P., Decarli, R., et al. 2016, ApJS, 227, 11

Bañados, E., Venemans, B. P., Mazzucchelli, C., et al. 2018, Nature, 553, 473

Badurina, L., Buchmueller, O., Ellis, J., et al. 2022, Philosophical Transactions of the Royal Society of London Series A, 380, 20210060

Badurina, L., Bentine, E., Blas, D., et al. 2020, JCAP, 2020, 011

Baillard, A., Bertin, E., de Lapparent, V., et al. 2011, A&A, 532, A74

Baker, W. M., Maiolino, R., Bluck, A. F. L., et al. 2023, arXiv e-prints, arXiv:2309.00670

Balcells, M., Graham, A. W., Domínguez-Palmero, L., & Peletier, R. F. 2003, ApJL, 582, L79

Baldassare, V. F., Stone, N. C., Foord, A., Gallo, E., & Ostriker, J. P. 2022, ApJ, 929, 84

Baldwin, J. A., Phillips, M. M., & Terlevich, R. 1981, PASP, 93, 5

Ballone, A., Mapelli, M., & Pasquato, M. 2018, MNRAS, 480, 4684

Ballone, A., Mapelli, M., & Pasquato, M. 2021, in Astronomical Society of the Pacific Conference Series, Vol. 528, New Horizons in Galactic Center Astronomy and Beyond, ed. M. Tsuboi & T. Oka, 175

Barai, P., & de Gouveia Dal Pino, E. M. 2019, MNRAS, 487, 5549

Bardati, J., Ruan, J. J., Haggard, D., & Tremmel, M. 2023, arXiv e-prints, arXiv:2308.03828

Barnes, E. I., & Sellwood, J. A. 2003, AJ, 125, 1164

Barrows, R. S., Mezcua, M., & Comerford, J. M. 2019, ApJ, 882, 181

Bear, E., & Soker, N. 2020, NewA, 81, 101438

Begelman, M. C., Volonteri, M., & Rees, M. J. 2006, MNRAS, 370, 289
Beifiori, A., Courteau, S., Corsini, E. M., & Zhu, Y. 2012, MNRAS, 419, 2497
Bellhouse, C., McGee, S. L., Smith, R., et al. 2021, MNRAS, 500, 1285
Bellovary, J. M., Cleary, C. E., Munshi, F., et al. 2019, MNRAS, 482, 2913
Bellovary, J. M., Hayoune, S., Chafla, K., et al. 2021, MNRAS, 505, 5129
Bennert, V. N., Auger, M. W., Treu, T., Woo, J.-H., & Malkan, M. A. 2011, ApJ, 726, 59
Bennett, J. S., Sijacki, D., Costa, T., Laporte, N., & Witten, C. 2024, MNRAS, 527, 1033
Berrier, J. C., Davis, B. L., Kennefick, D., et al. 2013, ApJ, 769, 132
Bhowmick, A. K., Blecha, L., Torrey, P., et al. 2022, MNRAS, 510, 177
Bi, S., Feng, H., & Ho, L. C. 2020, ApJ, 900, 124
Binggeli, B., Barazza, F., & Jerjen, H. 2000, A&A, 359, 447
Birchall, K. L., Watson, M. G., Aird, J., & Starling, R. L. C. 2022, MNRAS, 510, 4556
Blecha, L., Ivanova, N., Kalogera, V., et al. 2006, ApJ, 642, 427
Block, D. L., & Puerari, I. 1999, A&A, 342, 627
Bluck, A. F. L., Piotrowska, J. M., & Maiolino, R. 2023, ApJ, 944, 108
Boco, L., Lapi, A., & Danese, L. 2020, ApJ, 891, 94
Boehle, A., Ghez, A. M., Schödel, R., et al. 2016, ApJ, 830, 17
Bogdán, Á., Goulding, A. D., Natarajan, P., et al. 2023, Nature Astronomy
Bohn, T., Canalizo, G., Satyapal, S., & Pfeifle, R. W. 2020, ApJ, 899, 82
Bortolas, E., Ryu, T., Broggi, L., & Sesana, A. 2023, MNRAS, 524, 3026
Breiding, P., Chiaberge, M., Lambrides, E., et al. 2023, arXiv e-prints, arXiv:2305.11804
Bromm, V., & Loeb, A. 2003, ApJ, 596, 34
Burke, C. J., Shen, Y., Blaes, O., et al. 2021, Science, 373, 789
Burkert, A., & Tremaine, S. 2010, ApJ, 720, 516
Buta, R. J. 2014, in Astronomical Society of the Pacific Conference Series, Vol. 480, Structure and Dynamics of Disk Galaxies, ed. M. S. Seigar & P. Treuthardt, 53
Buta, R. J., Sheth, K., Regan, M., et al. 2010, ApJS, 190, 147
Buta, R. J., Sheth, K., Athanassoula, E., et al. 2015, ApJS, 217, 32
Cann, J. M., Satyapal, S., Abel, N. P., et al. 2018, ApJ, 861, 142
Cann, J. M., Satyapal, S., Rothberg, B., et al. 2021, ApJL, 912, L2
Chabrier, G. 2003, PASP, 115, 763
Chadayammuri, U., Bogdán, Á., Ricarte, A., & Natarajan, P. 2023, ApJ, 946, 51
Chakraborty, S., Gallerani, S., Zana, T., et al. 2023, MNRAS, 523, 758
Chambers, K. C., Magnier, E. A., Metcalfe, N., et al. 2016, arXiv e-prints, arXiv:1612.05560
Charbonnel, C., Schaerer, D., Prantzos, N., et al. 2023, A&A, 673, L7
Chassonnery, P., & Capuzzo-Dolcetta, R. 2021, MNRAS, 504, 3909
Chattopadhyay, D., Stegmann, J., Antonini, F., Barber, J., & Romero-Shaw, I. M. 2023, MNRAS, 526, 4908
Chen, B.-Y., Bower, G. C., Dexter, J., et al. 2023a, ApJ, 951, 93
Chen, J.-H., Shen, R.-F., & Liu, S.-F. 2023b, ApJ, 947, 32
Chen, Q.-H., Grasha, K., Battisti, A. J., et al. 2023c, MNRAS
Chen, W.-C. 2020, ApJ, 896, 129
Chen, Y.-C., Liu, X., Foord, A., et al. 2023d, Nature, 616, 45
Chen, Z.-C., Yuan, C., & Huang, Q.-G. 2022, Physics Letters B, 829, 137040
Cheng, R. M., & Bogdanović, T. 2014, PhRvD, 90, 064020
Chilingarian, I. V., Katkov, I. Y., Zolotukhin, I. Y., et al. 2018, ApJ, 863, 1
Chilingarian, I. V., Zolotukhin, I. Y., Katkov, I. Y., et al. 2017, ApJS, 228, 14
Cho, H., Woo, J.-H., Wang, S., et al. 2023, ApJ, 953, 142
Chu, A., Boldrini, P., & Silk, J. 2023, MNRAS, 522, 948
Chugunov, I. V., Mosenkov, A. V., Marchuk, A. A., et al. 2023, arXiv e-prints, arXiv:2311.01848
Cisternas, M., Jahnke, K., Inskip, K. J., et al. 2011, ApJ, 726, 57
Clausen, D., & Eracleous, M. 2011, ApJ, 726, 34
Clesse, S., & García-Bellido, J. 2015, PhRvD, 92, 023524
Comerford, J. M., Negus, J., Barrows, R. S., et al. 2022, ApJ, 927, 23
Costa, G., Mapelli, M., Iorio, G., et al. 2023, MNRAS, 525, 2891
Costantin, L., Pérez-González, P. G., Guo, Y., et al. 2023, arXiv e-prints, arXiv:2311.04283
Coughlin, E. R., & Nicholl, M. 2023, ApJL, 948, L22
Coughlin, E. R., & Nixon, C. J. 2022, ApJ, 936, 70
Cranmer, M. 2023, arXiv e-prints, arXiv:2305.01582

Curtis-Lake, E., Carniani, S., Cameron, A., et al. 2023, Nature Astronomy

Daniels, G. 1952, The Average Man?, Technical note WCRD (Wright-Patterson Air Force Base). https://books.google.com.au/books?id=NxmdHAAACAAJ

Das, A., Schleicher, D. R. G., Basu, S., & Boekholt, T. C. N. 2021, MNRAS, 505, 2186

Davies, M. B., Miller, M. C., & Bellovary, J. M. 2011, ApJL, 740, L42

Davis, B. 2015, PhD thesis, University of Arkansas

Davis, B. L., Berrier, J. C., Shields, D. W., et al. 2012, ApJS, 199, 33

—. 2016, 2DFFT: Measuring Galactic Spiral Arm Pitch Angle

Davis, B. L., Graham, A., Sahu, N., & Cameron, E. 2019a, in American Astronomical Society Meeting Abstracts, Vol. 234, American Astronomical Society Meeting Abstracts #234, 215.04

Davis, B. L., & Graham, A. W. 2021, PASA, 38, e030

Davis, B. L., Graham, A. W., & Cameron, E. 2018, ApJ, 869, 113

—. 2019b, ApJ, 873, 85

Davis, B. L., Graham, A. W., & Combes, F. 2019c, ApJ, 877, 64

Davis, B. L., Graham, A. W., & Seigar, M. S. 2017, MNRAS, 471, 2187

Davis, B. L., & Jin, Z. 2023, ApJL, 956, L22

Davis, B. L., Sahu, N., & Graham, A. W. 2021, in Galaxy Evolution and Feedback across Different Environments, ed. T. Storchi Bergmann, W. Forman, R. Overzier, & R. Riffel, Vol. 359, 37–39

Davis, B. L., Berrier, J. C., Johns, L., et al. 2014, ApJ, 789, 124

Davis, B. L., Kennefick, D., Kennefick, J., et al. 2015, ApJL, 802, L13

Davis, D. R., & Hayes, W. B. 2014, ApJ, 790, 87

Davis, F., Kaviraj, S., Hardcastle, M. J., et al. 2022, MNRAS, 511, 4109

Davoudiasl, H., Denton, P. B., & Gehrlein, J. 2022, PhRvL, 128, 081101

de Lapparent, V., Baillard, A., & Bertin, E. 2011, A&A, 532, A75

de Nicola, S., Marconi, A., & Longo, G. 2019, MNRAS, 490, 600

de Vaucouleurs, G. 1959, Handbuch der Physik, 53, 275

de Vaucouleurs, G., de Vaucouleurs, A., Corwin, Herold G., J., et al. 1991, Third Reference Catalogue of Bright Galaxies (Springer, New York)

Decarli, R., Walter, F., Venemans, B. P., et al. 2018, ApJ, 854, 97

Dekel, A., Sarkar, K. C., Birnboim, Y., Mandelker, N., & Li, Z. 2023, MNRAS, 523, 3201

den Brok, M., Peletier, R. F., Seth, A., et al. 2014, MNRAS, 445, 2385

Di Carlo, U. N., Mapelli, M., Pasquato, M., et al. 2021, MNRAS, 507, 5132

Di Cintio, P., Pasquato, M., Barbieri, L., Trani, A. A., & di Carlo, U. N. 2023, A&A, 673, A8

Di Matteo, T., Angles-Alcazar, D., & Shankar, F. 2023a, arXiv e-prints, arXiv:2304.11541

Di Matteo, T., Ni, Y., Chen, N., et al. 2023b, MNRAS, 525, 1479

Díaz-García, S., Salo, H., Knapen, J. H., & Herrera-Endoqui, M. 2019, A&A, 631, A94

Dickson, N., Smith, P. J., Hénault-Brunet, V., Gieles, M., & Baumgardt, H. 2023, arXiv e-prints, arXiv:2308.13037

Dijkstra, M., Ferrara, A., & Mesinger, A. 2014, MNRAS, 442, 2036

Dobbs, C., & Baba, J. 2014, PASA, 31, e035

Dong, X., Wang, T., Yuan, W., et al. 2007, ApJ, 657, 700

Dong-Páez, C. A., Volonteri, M., Beckmann, R. S., et al. 2023a, A&A, 676, A2

—. 2023b, A&A, 676, A2

D'Onghia, E., & Burkert, A. 2004, ApJL, 612, L13

D'Onofrio, M., Marziani, P., & Chiosi, C. 2021, Frontiers in Astronomy and Space Sciences, 8, 157

Driver, S. P., Bellstedt, S., Robotham, A. S. G., et al. 2022, MNRAS, 513, 439

Dullo, B. T., Bouquin, A. Y. K., Gil de Paz, A., Knapen, J. H., & Gorgas, J. 2020, ApJ, 898, 83

Dumont, A., Seth, A. C., Strader, J., et al. 2022, ApJ, 929, 147

Ebisuzaki, T., Makino, J., Tsuru, T. G., et al. 2001, ApJL, 562, L19

Einstein, A. 1916, Sitzungsberichte der Königlich Preußischen Akademie der Wissenschaften (Berlin, 688

Ellison, S. L., Patton, D. R., Mendel, J. T., & Scudder, J. M. 2011, MNRAS, 418, 2043

Endsley, R., Stark, D. P., Lyu, J., et al. 2023, MNRAS, 520, 4609

Escala, A. 2021, ApJ, 908, 57

Eskridge, P. B., Frogel, J. A., Pogge, R. W., et al. 2002, ApJS, 143, 73

Evans, M., Adhikari, R. X., Afle, C., et al. 2021, arXiv e-prints, arXiv:2109.09882

Event Horizon Telescope Collaboration, Akiyama, K., Alberdi, A., et al. 2019, ApJL, 875, L1

—. 2022, ApJL, 930, L12

Falcke, H., Körding, E., & Markoff, S. 2004, A&A, 414, 895

Fan, X., Narayanan, V. K., Lupton, R. H., et al. 2001, AJ, 122, 2833
Fan, X., Strauss, M. A., Schneider, D. P., et al. 2003, AJ, 125, 1649
Farrell, S. A., Webb, N. A., Barret, D., Godet, O., & Rodrigues, J. M. 2009, Nature, 460, 73
Farrell, S. A., Servillat, M., Pforr, J., et al. 2012, ApJL, 747, L13
Ferrara, A., Salvadori, S., Yue, B., & Schleicher, D. 2014, MNRAS, 443, 2410
Ferrarese, L. 2002, ApJ, 578, 90
Ferrarese, L., & Merritt, D. 2000, ApJL, 539, L9
Ferrarese, L., Côté, P., Sánchez-Janssen, R., et al. 2016, ApJ, 824, 10
Ferré-Mateu, A., Mezcua, M., & Barrows, R. S. 2021, MNRAS, 506, 4702
Fishbach, M., & Holz, D. E. 2020, ApJL, 904, L26
Fragione, G. 2022, ApJ, 939, 97
Fragione, G., Kocsis, B., Rasio, F. A., & Silk, J. 2022a, ApJ, 927, 231
Fragione, G., & Loeb, A. 2023, ApJ, 944, 81
Fragione, G., Loeb, A., Kocsis, B., & Rasio, F. A. 2022b, ApJ, 933, 170
Fragione, G., Loeb, A., Kremer, K., & Rasio, F. A. 2020a, ApJ, 897, 46
Fragione, G., Loeb, A., & Rasio, F. A. 2020b, ApJL, 902, L26
Fragione, G., & Silk, J. 2020, MNRAS, 498, 4591
Fridman, A. M., & Poltorak, S. G. 2010, MNRAS, 403, 1625
Fryer, C. L., Woosley, S. E., & Heger, A. 2001, ApJ, 550, 372
Fusco, M. S., Davis, B. L., Kennefick, J., Kennefick, D., & Seigar, M. S. 2022, Universe, 8, 649
Gair, J. R. 2009, Classical and Quantum Gravity, 26, 094034
Gair, J. R., Tang, C., & Volonteri, M. 2010, PhRvD, 81, 104014
Gallo, E., & Sesana, A. 2019, ApJL, 883, L18
Gao, F., Wang, L., Pearson, W. J., et al. 2020, A&A, 637, A94
García-Gómez, C., Barberà, C., Athanassoula, E., Bosma, A., & Whyte, L. 2004, A&A, 421, 595
Gardner, J. P., Mather, J. C., Clampin, M., et al. 2006, SSRv, 123, 485
Gebhardt, K., Bender, R., Bower, G., et al. 2000, ApJL, 539, L13
Gelli, V., Salvadori, S., Ferrara, A., Pallottini, A., & Carniani, S. 2023, ApJL, 954, L11
Georgiev, I. Y., & Böker, T. 2014, MNRAS, 441, 3570
Georgiev, I. Y., Böker, T., Leigh, N., Lützgendorf, N., & Neumayer, N. 2016, MNRAS, 457, 2122
Gezari, S. 2021, ARA&A, 59, 21
Giani, L., Howlett, C., & Davis, T. M. 2023, The Open Journal of Astrophysics, 6, 26
Gomez, S., & Gezari, S. 2023, ApJ, 955, 46
Gong, J.-Y., Mao, Y.-W., Gao, H., & Yu, S.-Y. 2023, ApJS, 267, 26
González-López lira, R. A., Lomelí-Núñez, L., Ordenes-Briceño, Y., et al. 2022, ApJ, 941, 53
González-Martín, O., & Vaughan, S. 2012, A&A, 544, A80
Goradzhanov, V., Chilingarian, I., Katkov, I., et al. 2022, in Astronomy at the Epoch of Multimessenger Studies, 367–369
Goulding, A. D., & Greene, J. E. 2022, ApJL, 938, L9
Goulding, A. D., Greene, J. E., Bezanson, R., et al. 2018, PASJ, 70, S37
Goulding, A. D., Greene, J. E., Setton, D. J., et al. 2023, ApJL, 955, L24
Graham, A. W. 2003, AJ, 125, 3398
—. 2016a, Astrophysics and Space Science Library, Vol. 418, Galaxy Bulges and Their Massive Black Holes: A Review (Springer International Publishing Switzerland), 263
Graham, A. W. 2016b, in IAU Symposium, Vol. 312, Star Clusters and Black Holes in Galaxies across Cosmic Time, ed. Y. Meiron, S. Li, F. K. Liu, & R. Spurzem, 269–273
—. 2019, MNRAS, 487, 4995
—. 2020, MNRAS, 492, 3263
—. 2023a, MNRAS, 522, 3588
—. 2023b, MNRAS, 521, 1023
—. 2023c, MNRAS, 518, 6293
Graham, A. W., Driver, S. P., Allen, P. D., & Liske, J. 2007, MNRAS, 378, 198
Graham, A. W., & Sahu, N. 2023a, MNRAS, 520, 1975
—. 2023b, MNRAS, 518, 2177
Graham, A. W., & Scott, N. 2013, ApJ, 764, 151
Graham, A. W., Scott, N., & Schombert, J. M. 2015, Publication of Korean Astronomical Society, 30, 335
Graham, A. W., & Soria, R. 2019, MNRAS, 484, 794
Graham, A. W., Soria, R., Ciambur, B. C., Davis, B. L., & Swartz, D. A. 2021a, ApJ, 923, 146
Graham, A. W., Soria, R., & Davis, B. L. 2019, MNRAS, 484, 814
Graham, A. W., Soria, R., Davis, B. L., et al. 2021b, ApJ, 923, 246
Graham, A. W., & Spitler, L. R. 2009, MNRAS, 397, 2148
Graham, A. W., & Worley, C. C. 2008, MNRAS, 388, 1708

Gravity Collaboration, Abuter, R., Amorim, A., et al. 2020, A&A, 636, L5
Graziani, R., Courtois, H. M., Lavaux, G., et al. 2019, MNRAS, 488, 5438
Greene, J. E. 2012, Nature Communications, 3, 1304
Greene, J. E., Strader, J., & Ho, L. C. 2020, ARA&A, 58, 257
Grosbøl, P. J. 1985, A&AS, 60, 261
Gültekin, K., Nyland, K., Gray, N., et al. 2022, MNRAS, 516, 6123
Guo, Y., Jogee, S., Finkelstein, S. L., et al. 2023, ApJL, 945, L10
Gürkan, M. A., Fregeau, J. M., & Rasio, F. A. 2006, ApJL, 640, L39
Guzmán-Ortega, A., Rodriguez-Gomez, V., Snyder, G. F., Chamberlain, K., & Hernquist, L. 2023, MNRAS, 519, 4920
Haas, R., Shcherbakov, R. V., Bode, T., & Laguna, P. 2012, ApJ, 749, 117
Habouzit, M., Volonteri, M., Latif, M., Dubois, Y., & Peirani, S. 2016a, MNRAS, 463, 529
Habouzit, M., Volonteri, M., Latif, M., et al. 2016b, MNRAS, 456, 1901
Haemmerlé, L., Klessen, R. S., Mayer, L., & Zwick, L. 2021, A&A, 652, L7
Haemmerlé, L., Mayer, L., Klessen, R. S., et al. 2020, SSRv, 216, 48
Haemmerlé, L., Woods, T. E., Klessen, R. S., Heger, A., & Whalen, D. J. 2018a, ApJL, 853, L3
—. 2018b, MNRAS, 474, 2757
Haidar, H., Habouzit, M., Volonteri, M., et al. 2022, MNRAS, 514, 4912
Haiman, Z., & Loeb, A. 2001, ApJ, 552, 459
Haiman, Z., Xin, C., Bogdanović, T., et al. 2023, arXiv e-prints, arXiv:2306.14990
Harris, C. R., Millman, K. J., van der Walt, S. J., et al. 2020, Nature, 585, 357–362
Harris, G. L. H., & Harris, W. E. 2011, MNRAS, 410, 2347
Harris, G. L. H., Poole, G. B., & Harris, W. E. 2014, MNRAS, 438, 2117
Harry, G. M., & LIGO Scientific Collaboration. 2010, Classical and Quantum Gravity, 27, 084006
Hart, R. E., Bamford, S. P., Keel, W. C., et al. 2018, MNRAS, 478, 932
Hart, R. E., Bamford, S. P., Hayes, W. B., et al. 2017, MNRAS, 472, 2263
Hatano, S., Ouchi, M., Nakajima, K., et al. 2023a, arXiv e-prints, arXiv:2304.03726
Hatano, S., Ouchi, M., Umeda, H., et al. 2023b, arXiv e-prints, arXiv:2305.02189
Heger, A., Fryer, C. L., Woosley, S. E., Langer, N., & Hartmann, D. H. 2003, ApJ, 591, 288
Hénault-Brunet, V., Gieles, M., Strader, J., et al. 2020, MNRAS, 491, 113
Herenz, E. C., Micheva, G., Weilbacher, P. M., et al. 2023, Research Notes of the AAS, 7, 99
Hernández-Toledo, H. M., Cortes-Suárez, E., Vázquez-Mata, J. A., et al. 2023, MNRAS, 523, 4164
Herrera-Endoqui, M., Díaz-García, S., Laurikainen, E., & Salo, H. 2015, A&A, 582, A86
Hijikawa, K., Tanikawa, A., Kinugawa, T., Yoshida, T., & Umeda, H. 2021, MNRAS, 505, L69
Hills, J. G. 1975, Nature, 254, 295
Hirano, S., Machida, M. N., & Basu, S. 2021, ApJ, 917, 34
Ho, L. C., Li, Z.-Y., Barth, A. J., Seigar, M. S., & Peng, C. Y. 2011, The Astrophysical Journal Supplement Series, 197, 21
Holley-Bockelmann, K., Micic, M., Sigurdsson, S., & Rubbo, L. J. 2010, ApJ, 713, 1016
Hon, D. S. H., Graham, A. W., Davis, B. L., & Marconi, A. 2022, MNRAS, 514, 3410
Hon, D. S. H., Graham, A. W., & Sahu, N. 2023, MNRAS, 519, 4651
Hong, J., Im, M., Kim, M., & Ho, L. C. 2015, ApJ, 804, 34
Hooper, D., Ireland, A., Krnjaic, G., & Stebbins, A. 2023, arXiv e-prints, arXiv:2308.00756
Hopkins, P. F., Hernquist, L., Cox, T. J., et al. 2006, ApJS, 163, 1
Hosokawa, T., Yorke, H. W., Inayoshi, K., Omukai, K., & Yoshida, N. 2013, ApJ, 778, 178
Huang, S., Kawabe, R., Kohno, K., et al. 2023, arXiv e-prints, arXiv:2310.01782
Hubble, E. 1926a, Contributions from the Mount Wilson Observatory / Carnegie Institution of Washington, 324, 1
Hubble, E. P. 1926b, ApJ, 64, 321
—. 1927, The Observatory, 50, 276
—. 1936, Realm of the Nebulae (New Haven: Yale University Press)
Hunter, J. D. 2007, Computing in Science & Engineering, 9, 90–95
Inayoshi, K., Visbal, E., & Haiman, Z. 2020, ARA&A, 58, 27
Ito, K., Valentino, F., Brammer, G., et al. 2023, arXiv e-prints, arXiv:2307.06994
Izquierdo-Villalba, D., Colpi, M., Volonteri, M., et al. 2023, A&A, 677, A123
Jani, K., Shoemaker, D., & Cutler, C. 2020, Nature Astronomy, 4, 260
Jeans, J. H. 1919, Problems of cosmogony and stellar dynamics (Cambridge, University press)

—. 1928, Astronomy and cosmogony (Cambridge [Eng.] The University press)
Jeon, J., Liu, B., Bromm, V., & Finkelstein, S. L. 2023, MNRAS, 524, 176
Jerjen, H., Kalnajs, A., & Binggeli, B. 2000, A&A, 358, 845
Jiang, Y.-F., Stone, J. M., & Davis, S. W. 2019, ApJ, 880, 67
Jin, Z., & Davis, B. L. 2023, arXiv e-prints, arXiv:2310.19406
Johnson, J. L., & Upton Sanderbeck, P. R. 2022, ApJ, 934, 58
Jorgensen, I., Franx, M., & Kjaergaard, P. 1995, MNRAS, 276, 1341
Joseph, T. D., Maccarone, T. J., & Fender, R. P. 2011, MNRAS, 415, L59
Joye, W. A., & Mandel, E. 2003, in Astronomical Society of the Pacific Conference Series, Vol. 295, Astronomical Data Analysis Software and Systems XII, ed. H. E. Payne, R. I. Jedrzejewski, & R. N. Hook, 489
Kaaret, P., Prestwich, A. H., Zezas, A., et al. 2001, MNRAS, 321, L29
Kains, N., Bramich, D. M., Sahu, K. C., & Calamida, A. 2016, MNRAS, 460, 2025
Kalirai, J. 2018, Contemporary Physics, 59, 251
Karachentsev, I. D., & Karachentseva, V. E. 2019, MNRAS, 485, 1477
Karouzos, M., Jarvis, M. J., & Bonfield, D. 2014, MNRAS, 439, 861
Kartaltepe, J. S., Rose, C., Vanderhoof, B. N., et al. 2023, ApJL, 946, L15
Kashikawa, N., Ishizaki, Y., Willott, C. J., et al. 2015, ApJ, 798, 28
Kauffmann, G., & Haehnelt, M. 2000, MNRAS, 311, 576
Kendall, S., Clarke, C., & Kennicutt, R. C. 2015, MNRAS, 446, 4155
Kennicutt, R. C., J. 1981, AJ, 86, 1847
Kewley, L. J., Groves, B., Kauffmann, G., & Heckman, T. 2006, MNRAS, 372, 961
Khan, F. M., & Holley-Bockelmann, K. 2021, MNRAS, 508, 1174
Kim, J., Lee, J., Laigle, C., et al. 2023, ApJ, 951, 137
Kim, M., Ho, L. C., & Im, M. 2017, ApJL, 844, L21
Kim, M., López, K. M., Jonker, P. G., Ho, L. C., & Im, M. 2020, MNRAS, 493, L76
Kim, M., Ho, L. C., Wang, J., et al. 2015, ApJ, 814, 8
Kıroğlu, F., Lombardi, J. C., Kremer, K., et al. 2023, ApJ, 948, 89
Kızıltan, B., Baumgardt, H., & Loeb, A. 2017, Nature, 542, 203
Kobayashi, S., Laguna, P., Phinney, E. S., & Mészáros, P. 2004, ApJ, 615, 855
Kocevski, D. D., Faber, S. M., Mozena, M., et al. 2012, ApJ, 744, 148
Kocevski, D. D., Onoue, M., Inayoshi, K., et al. 2023, ApJL, 954, L4
Kojima, T., Ouchi, M., Rauch, M., et al. 2021, ApJ, 913, 22
Koliopanos, F. 2017, in XII Multifrequency Behaviour of High Energy Cosmic Sources Workshop (MULTIF2017), 51
Koliopanos, F., Ciambur, B. C., Graham, A. W., et al. 2017, A&A, 601, A20
Kolmogorov, A. 1933, G. Ist. Ital. Attuari, 4, 83
Koss, M., Mushotzky, R., Veilleux, S., & Winter, L. 2010, ApJL, 716, L125
Kourkchi, E., Courtois, H. M., Graziani, R., et al. 2020, AJ, 159, 67
Kovetz, E. D., Cholis, I., Kamionkowski, M., & Silk, J. 2018, PhRvD, 97, 123003
Kroupa, P., Subr, L., Jerabkova, T., & Wang, L. 2020, MNRAS, 498, 5652
Labbé, I., van Dokkum, P., Nelson, E., et al. 2023, Nature, 616, 266
Lacerda, E. A. D., Sánchez, S. F., Cid Fernandes, R., et al. 2020, MNRAS, 492, 3073
Laghi, D., Tamanini, N., Del Pozzo, W., et al. 2021, MNRAS, 508, 4512
Lam, C. Y., Lu, J. R., Udalski, A., et al. 2022, ApJL, 933, L23
Lambrides, E. L., Chiaberge, M., Heckman, T., et al. 2021, ApJ, 919, 129
Lanfranchi, G. A., Hazenfratz, R., Caproni, A., & Silk, J. 2021, ApJ, 914, 32
Larson, R. L., Finkelstein, S. L., Kocevski, D. D., et al. 2023, ApJL, 953, L29
Latif, M. A., Khochfar, S., Schleicher, D., & Whalen, D. J. 2021, MNRAS, 508, 1756
Latif, M. A., Khochfar, S., & Whalen, D. 2020, ApJL, 892, L4
Laurikainen, E., Salo, H., Buta, R., & Knapen, J. H. 2007, MNRAS, 381, 401
Lee, S., Kim, J.-h., & Oh, B. K. 2023, ApJ, 943, 77
Leveque, A., Giersz, M., Askar, A., Arca-Sedda, M., & Olejak, A. 2023, MNRAS, 520, 2593
Li, W., Inayoshi, K., & Qiu, Y. 2021, ApJ, 917, 60
Li, W., Inayoshi, K., Onoue, M., et al. 2023, arXiv e-prints, arXiv:2306.06172
Li, X.-D. 2004, ApJL, 616, L119
LIGO Scientific Collaboration, Aasi, J., Abbott, B. P., et al. 2015, Classical and Quantum Gravity, 32, 074001

Lin, C. C., & Shu, F. H. 1966, Proceedings of the National Academy of Science, 55, 229
Lin, C.-H., Chen, K.-J., & Hwang, C.-Y. 2023, ApJ, 952, 121
Lin, D., Carrasco, E. R., Webb, N. A., et al. 2016, ApJ, 821, 25
Lin, D., Strader, J., Romanowsky, A. J., et al. 2020a, ApJL, 892, L25
—. 2020b, ApJL, 892, L25
Lingard, T., Masters, K. L., Krawczyk, C., et al. 2021, MNRAS, 504, 3364
Lisker, T., Grebel, E. K., & Binggeli, B. 2006, AJ, 132, 497
Lodato, G., & Natarajan, P. 2006, MNRAS, 371, 1813
Loeb, A., & Rasio, F. A. 1994, ApJ, 432, 52
Looser, T. J., D'Eugenio, F., Maiolino, R., et al. 2023a, arXiv e-prints, arXiv:2306.02470
—. 2023b, arXiv e-prints, arXiv:2302.14155
Luminet, J. P., & Pichon, B. 1989, A&A, 209, 103
Lundmark, K. 1925, MNRAS, 85, 865
Lupi, A., Colpi, M., Devecchi, B., Galanti, G., & Volonteri, M. 2014, MNRAS, 442, 3616
Lupi, A., Haiman, Z., & Volonteri, M. 2021, MNRAS, 503, 5046
Ma, J. 2001, ChJA&A, 1, 395
Ma, J., Zhao, J. L., Shu, C. G., & Peng, Q. H. 1999, A&A, 350, 31
Ma, L., Hopkins, P. F., Ma, X., et al. 2021, MNRAS, 508, 1973
MacLeod, M., Guillochon, J., & Ramirez-Ruiz, E. 2012, ApJ, 757, 134
MacLeod, M., Guillochon, J., Ramirez-Ruiz, E., Kasen, D., & Rosswog, S. 2016, ApJ, 819, 3
Madau, P., Haardt, F., & Dotti, M. 2014, ApJL, 784, L38
Madau, P., & Rees, M. J. 2001, ApJL, 551, L27
Magorrian, J., Tremaine, S., Richstone, D., et al. 1998, AJ, 115, 2285
Maguire, K., Eracleous, M., Jonker, P. G., MacLeod, M., & Rosswog, S. 2020, SSRv, 216, 39
Mahani, H., Zonoozi, A. H., Haghi, H., et al. 2021, MNRAS, 502, 5185
Maiolino, R., Scholtz, J., Curtis-Lake, E., et al. 2023a, arXiv e-prints, arXiv:2308.01230
Maiolino, R., Scholtz, J., Witstok, J., et al. 2023b, arXiv e-prints, arXiv:2305.12492
Makarov, D., Prugniel, P., Terekhova, N., Courtois, H., & Vauglin, I. 2014, A&A, 570, A13
Mangiagli, A., Caprini, C., Volonteri, M., et al. 2022, PhRvD, 106, 103017
Mapelli, M., Ripamonti, E., Vecchio, A., Graham, A. W., & Gualandris, A. 2012a, A&A, 542, A102
Mapelli, M., Santoliquido, F., Bouffanais, Y., et al. 2021a, Symmetry, 13, 1678
Mapelli, M., Zampieri, L., & Mayer, L. 2012b, MNRAS, 423, 1309
Mapelli, M., Dall'Amico, M., Bouffanais, Y., et al. 2021b, MNRAS, 505, 339
Martínez-García, E. E., González-López lira, R. A., & Puerari, I. 2023, MNRAS, 524, 18
Massonneau, W., Volonteri, M., Dubois, Y., & Beckmann, R. S. 2023, A&A, 670, A180
Masters, K. L., Lintott, C. J., Hart, R. E., et al. 2019, MNRAS, 487, 1808
Matsumoto, H., Tsuru, T. G., Koyama, K., et al. 2001, ApJL, 547, L25
Matsuoka, Y., Iwasawa, K., Onoue, M., et al. 2019, ApJ, 883, 183
Matsushita, S., Kawabe, R., Matsumoto, H., et al. 2000, ApJL, 545, L107
Mayes, R., Drinkwater, M., Pfeffer, J., & Baumgardt, H. 2023, arXiv e-prints, arXiv:2302.08082
McKernan, B., Ford, K. E. S., Lyra, W., & Perets, H. B. 2012, MNRAS, 425, 460
McKinney, W. 2010, in Proceedings of the 9th Python in Science Conference, Vol. 445, Austin, TX, 51–56
Medeiros, L., Psaltis, D., Lauer, T. R., & Özel, F. 2023, ApJL, 947, L7
Mengistu, P., & Masters, K. L. 2023, Research Notes of the American Astronomical Society, 7, 35
Merloni, A., Heinz, S., & di Matteo, T. 2003, MNRAS, 345, 1057
Mezcua, M. 2017, International Journal of Modern Physics D, 26, 1730021
Mezcua, M., Civano, F., Fabbiano, G., Miyaji, T., & Marchesi, S. 2016, ApJ, 817, 20
Mezcua, M., Civano, F., Marchesi, S., et al. 2018, MNRAS, 478, 2576
Mezcua, M., & Domínguez Sánchez, H. 2020, ApJL, 898, L30
Mezcua, M., Roberts, T. P., Lobanov, A. P., & Sutton, A. D. 2015, MNRAS, 448, 1893
Mezcua, M., Siudek, M., Suh, H., et al. 2023, ApJL, 943, L5
Michea, J., Pasquali, A., Smith, R., et al. 2021, AJ, 161, 268
Mićić, M., Irwin, J. A., & Lin, D. 2022, ApJ, 928, 117
Miller, B. P., Gallo, E., Greene, J. E., et al. 2015, ApJ, 799, 98
Miller, R., Kennefick, D., Kennefick, J., et al. 2019, ApJ, 874, 177
Molina, M., Reines, A. E., Latimer, L. J., Baldassare, V., & Salehirad, S. 2021, ApJ, 922, 155

Morganson, E., De Rosa, G., Decarli, R., et al. 2012, AJ, 143, 142
Moriya, T. J., Chen, K.-J., Nakajima, K., Tominaga, N., & Blinnikov, S. I. 2021, MNRAS, 503, 1206
Mortlock, D. J., Warren, S. J., Venemans, B. P., et al. 2011, Nature, 474, 616
Morton, S., Rinaldi, S., Torres-Orjuela, A., et al. 2023, arXiv e-prints, arXiv:2310.16025
Mutlu-Pakdil, B., Seigar, M. S., & Davis, B. L. 2016, ApJ, 830, 117
Muxlow, T. W. B., Beswick, R. J., Garrington, S. T., et al. 2010, MNRAS, 404, L109
Nakajima, K., & Maiolino, R. 2022, MNRAS, 513, 5134
Natarajan, P. 2021, MNRAS, 501, 1413
Natarajan, P., Pacucci, F., Ferrara, A., et al. 2017, ApJ, 838, 117
Natarajan, P., Pacucci, F., Ricarte, A., et al. 2023, arXiv e-prints, arXiv:2308.02654
Navarro-Carrera, R., Rinaldi, P., Caputi, K. I., et al. 2023, arXiv e-prints, arXiv:2305.16141
Neumayer, N., Seth, A., & Böker, T. 2020, A&A Rv, 28, 4
Nguyen, D. D., Seth, A. C., Neumayer, N., et al. 2019, ApJ, 872, 104
Nicholl, M., Lanning, D., Ramsden, P., et al. 2022, MNRAS, 515, 5604
Nitz, A. H., & Capano, C. D. 2021, ApJL, 907, L9
Noyola, E., Gebhardt, K., & Bergmann, M. 2008, ApJ, 676, 1008
Nwaokoro, E., Phillipps, S., Young, A. J., et al. 2021, MNRAS, 502, 3101
O'Brien, B., Szczepańczyk, M., Gayathri, V., et al. 2021, PhRvD, 104, 082003
Ogata, E., Ohsuga, K., & Yajima, H. 2021, PASJ
Ohkubo, T., Umeda, H., Maeda, K., et al. 2006, ApJ, 645, 1352
Ohlson, D., Seth, A. C., Gallo, E., Baldassare, V. F., & Greene, J. E. 2023, arXiv e-prints, arXiv:2309.05701
Oka, T., Tsujimoto, S., Iwata, Y., Nomura, M., & Takekawa, S. 2017, Nature Astronomy, 1, 709
Ono, Y., Harikane, Y., Ouchi, M., et al. 2023, arXiv e-prints, arXiv:2309.02790
Onoue, M., Kashikawa, N., Matsuoka, Y., et al. 2019, ApJ, 880, 77
Ormerod, K., Conselice, C. J., Adams, N. J., et al. 2023, arXiv e-prints, arXiv:2309.04377
Overzier, R. A. 2022, ApJ, 926, 114
Pacucci, F., & Loeb, A. 2022, MNRAS, 509, 1885
Pacucci, F., Loeb, A., Mezcua, M., & Martín-Navarro, I. 2018, ApJL, 864, L6
Pacucci, F., Natarajan, P., Volonteri, M., Cappelluti, N., & Urry, C. M. 2017, ApJL, 850, L42
Pacucci, F., Nguyen, B., Carniani, S., Maiolino, R., & Fan, X. 2023a, ApJL, 957, L3
Pacucci, F., Seepaul, B., Ni, Y., Cappelluti, N., & Foord, A. 2023b, arXiv e-prints, arXiv:2311.08448
Pahre, M. A., Ashby, M. L. N., Fazio, G. G., & Willner, S. P. 2004, ApJS, 154, 235
Palmese, A., & Conselice, C. J. 2021, PhRvL, 126, 181103
Pan, H.-W., Yuan, W., Zhou, X.-L., Dong, X.-B., & Liu, B. 2015, ApJ, 808, 163
Panagiotou, C., De, K., Masterson, M., et al. 2023, ApJL, 948, L5
Partmann, C., Naab, T., Rantala, A., et al. 2023, arXiv e-prints, arXiv:2310.08079
Pasham, D. R., Strohmayer, T. E., & Mushotzky, R. F. 2014, Nature, 513, 74
Pasquato, M., Trevisan, P., Askar, A., et al. 2023, arXiv e-prints, arXiv:2310.18560
Patruno, A., Portegies Zwart, S., Dewi, J., & Hopman, C. 2006, MNRAS, 370, L6
Paynter, J., Webster, R., & Thrane, E. 2021, Nature Astronomy
Pechetti, R., Seth, A., Neumayer, N., et al. 2020, ApJ, 900, 32
Pechetti, R., Seth, A., Kamann, S., et al. 2022, ApJ, 924, 48
Peebles, P. J. E. 1972, ApJ, 178, 371
Peng, T. R., English, J. E., Silva, P., Davis, D. R., & Hayes, W. B. 2018, MNRAS, 479, 5532
Perley, D. A., Mazzali, P. A., Yan, L., et al. 2019, MNRAS, 484, 1031
Pfister, H., Volonteri, M., Dai, J. L., & Colpi, M. 2020, MNRAS, 497, 2276
Pfister, H., Volonteri, M., Dubois, Y., Dotti, M., & Colpi, M. 2019, MNRAS, 486, 101
Piro, L., Colpi, M., Aird, J., et al. 2023a, MNRAS, 521, 2577
—. 2023b, MNRAS, 521, 2577
Planck Collaboration, Aghanim, N., Akrami, Y., et al. 2020, A&A, 641, A6
Poltorak, S. G., & Fridman, A. M. 2007, Astronomy Reports, 51, 460
Portegies Zwart, S. F., Dewi, J., & Maccarone, T. 2004, MNRAS, 355, 413
Portegies Zwart, S. F., & McMillan, S. L. W. 2002, ApJ, 576, 899
Pour-Imani, H., Kennefick, D., Kennefick, J., et al. 2016, ApJL, 827, L2
Pringle, J. E., & Dobbs, C. L. 2019, MNRAS, 490, 1470

Qin, Y., Balu, S., & Wyithe, J. S. B. 2023, MNRAS, 526, 1324
Ramsden, P., Lanning, D., Nicholl, M., & McGee, S. L. 2022, MNRAS, 515, 1146
Rashkov, V., & Madau, P. 2014, ApJ, 780, 187
Raveh, Y., Ginat, Y. B., Perets, H. B., & Woods, T. E. 2021, MNRAS, 505, 3944
Reefe, M., Satyapal, S., Sexton, R. O., et al. 2022, ApJ, 936, 140
—. 2023, ApJL, 946, L38
Rees, M. J. 1988, Nature, 333, 523
Regan, J. A., Pacucci, F., & Bustamante-Rosell, M. J. 2023, MNRAS, 518, 5997
Reid, M. J., & Brunthaler, A. 2020, ApJ, 892, 39
Reines, A. E. 2022, Nature Astronomy, 6, 26
Reines, A. E., Condon, J. J., Darling, J., & Greene, J. E. 2020, ApJ, 888, 36
Reines, A. E., Greene, J. E., & Geha, M. 2013, ApJ, 775, 116
Reines, A. E., Sivakoff, G. R., Johnson, K. E., & Brogan, C. L. 2011, Nature, 470, 66
Renzo, M., Farmer, R., Justham, S., et al. 2020, A&A, 640, A56
Reshetnikov, V. P., Marchuk, A. A., Chugunov, I. V., Usachev, P. A., & Mosenkov, A. V. 2022, Astronomy Letters, 48, 644
Ricarte, A., & Natarajan, P. 2018, MNRAS, 481, 3278
Ricarte, A., Tremmel, M., Natarajan, P., Zimmer, C., & Quinn, T. 2021, MNRAS, 503, 6098
Rizzuto, F. P., Naab, T., Spurzem, R., et al. 2022, MNRAS, 512, 884
—. 2021, MNRAS, 501, 5257
Roberts, W. W., J., Roberts, M. S., & Shu, F. H. 1975, ApJ, 196, 381
Roberts, M. S. 1978, AJ, 83, 1026
Robertson, B. E., Tacchella, S., Johnson, B. D., et al. 2023, Nature Astronomy
Robotham, A. S. G., & Obreschkow, D. 2015, PASA, 32, e033
Robotham, A. S. G., & Obreschkow, D. 2016, Hyper-Fit: Fitting routines for multidimensional data with multivariate Gaussian uncertainties, Astrophysics Source Code Library, record ascl:1601.002
Rodriguez-Gomez, V., Genel, S., Fall, S. M., et al. 2022, MNRAS, 512, 5978
Rose, S. C., Naoz, S., Sari, R., & Linial, I. 2022, ApJL, 929, L22
Rosswog, S., Ramirez-Ruiz, E., & Hix, W. R. 2009, ApJ, 695, 404
Sabra, B. M., Saliba, C., Abi Akl, M., & Chahine, G. 2015, ApJ, 803, 5
Sahu, K. C., Anderson, J., Casertano, S., et al. 2022a, ApJ, 933, 83
Sahu, N. 2021, PhD thesis, Swinburne University of Technology, Australia
Sahu, N. 2022, in Hypatia Colloquium 2022, 24
Sahu, N., Graham, A. W., & Davis, B. L. 2019a, ApJ, 887, 10
—. 2019b, ApJ, 876, 155
—. 2020, ApJ, 903, 97
—. 2022b, Acta Astrophysica Taurica, 3, 39
—. 2022c, ApJ, 927, 67
Saini, P., Bhat, S. A., & Arun, K. G. 2022, PhRvD, 106, 104015
Salehirad, S., Reines, A. E., & Molina, M. 2022, ApJ, 937, 7
Sanchez, N. N., Werk, J. K., Christensen, C., et al. 2023, arXiv e-prints, arXiv:2305.07672
Sánchez-Janssen, R., Côté, P., Ferrarese, L., et al. 2019, ApJ, 878, 18
Sandage, A. 1961, The Hubble Atlas of Galaxies (Washington: Carnegie Institution)
Sandage, A., & Bedke, J. 1994, The Carnegie atlas of galaxies, Vol. 638 (Washington: Carnegie Institution)
Sarkar, S., Narayanan, G., Banerjee, A., & Prakash, P. 2023, MNRAS, 518, 1022
Sassano, F., Capelo, P. R., Mayer, L., Schneider, R., & Valiante, R. 2023, MNRAS, 519, 1837
Sassano, F., Schneider, R., Valiante, R., et al. 2021, MNRAS, 506, 613
Savchenko, S., Marchuk, A., Mosenkov, A., & Grishunin, K. 2020, MNRAS, 493, 390
Savorgnan, G., Graham, A. W., Marconi, A., et al. 2013, MNRAS, 434, 387
Savorgnan, G. A. D. 2016a, ApJ, 821, 88
—. 2016b, PhD thesis, Swinburne University of Technology, Australia
Savorgnan, G. A. D., Graham, A. W., Marconi, A., & Sani, E. 2016, ApJ, 817, 21
Schleicher, D. R. G., Reinoso, B., & Klessen, R. S. 2023, MNRAS, 521, 3972
Schleicher, D. R. G., Reinoso, B., Latif, M., et al. 2022, MNRAS, 512, 6192
Schödel, R., Eckart, A., Iserlohe, C., Genzel, R., & Ott, T. 2005, ApJL, 625, L111
Schutte, Z., & Reines, A. E. 2022, Nature, 601, 329
Scott, N., & Graham, A. W. 2013, ApJ, 763, 76
Secrest, N. J., Schmitt, H. R., Blecha, L., Rothberg, B., & Fischer, J. 2017, ApJ, 836, 183

Seigar, M. S., Block, D. L., Puerari, I., Chorney, N. E., & James, P. A. 2005, MNRAS, 359, 1065
Seigar, M. S., Bullock, J. S., Barth, A. J., & Ho, L. C. 2006, ApJ, 645, 1012
Seigar, M. S., Davis, B. L., Berrier, J., & Kennefick, D. 2014, ApJ, 795, 90
Seigar, M. S., & James, P. A. 1998, MNRAS, 299, 685
Seigar, M. S., Kennefick, D., Kennefick, J., & Lacy, C. H. S. 2008, ApJL, 678, L93
Sersic, J. L. 1968, Atlas de Galaxias Australes
Sesana, A., Gair, J., Berti, E., & Volonteri, M. 2011, PhRvD, 83, 044036
Sesana, A., Korsakova, N., Arca Sedda, M., et al. 2021, Experimental Astronomy, 51, 1333
Shankar, F., Salucci, P., Granato, G. L., De Zotti, G., & Danese, L. 2004, MNRAS, 354, 1020
Shankar, F., Weinberg, D. H., & Miralda-Escudé, J. 2009, ApJ, 690, 20
Shapley, H., & Paraskevopoulos, J. S. 1940, Proceedings of the National Academy of Science, 26, 31
Shaya, E. J., Tully, R. B., Hoffman, Y., & Pomarède, D. 2017, ApJ, 850, 207
Shen, X., Hopkins, P. F., Faucher-Giguère, C.-A., et al. 2020, MNRAS, 495, 3252
Sheth, K., Regan, M., Hinz, J. L., et al. 2010, PASP, 122, 1397
Shi, Y., Kremer, K., Grudić, M. Y., Gerling-Dunsmore, H. J., & Hopkins, P. F. 2023, MNRAS, 518, 3606
Shields, D., Boe, B., Pfountz, C., et al. 2022, Galaxies, 10, 100
Shields, D. W., Boe, B., Pfountz, C., et al. 2015, Spirality: Spiral arm pitch angle measurement
Silk, J. 2017, ApJL, 839, L13
Simien, F., & de Vaucouleurs, G. 1986, ApJ, 302, 564
Small, T. A., & Blandford, R. D. 1992, MNRAS, 259, 725
Smethurst, R. J., Simmons, B. D., Coil, A., et al. 2021, MNRAS, 507, 3985
Smethurst, R. J., Beckmann, R. S., Simmons, B. D., et al. 2023, MNRAS
Smirnov, N. 1948, The Annals of Mathematical Statistics, 19, 279 – 281
Smith, D., Haberzettl, L., Porter, L. E., et al. 2022, MNRAS, 517, 4575
Smith, M. D., Bureau, M., Davis, T. A., et al. 2021a, MNRAS, 500, 1933
Smith, R., Michea, J., Pasquali, A., et al. 2021b, ApJ, 912, 149
Soltan, A. 1982, MNRAS, 200, 115
Soria, R., Hakala, P. J., Hau, G. K. T., Gladstone, J. C., & Kong, A. K. H. 2012, MNRAS, 420, 3599
Soria, R., Hau, G. K. T., Graham, A. W., et al. 2010, MNRAS, 405, 870
Soria, R., Hau, G. K. T., & Pakull, M. W. 2013, ApJL, 768, L22
Soria, R., Zampieri, L., Zane, S., & Wu, K. 2011, MNRAS, 410, 1886
Soria, R., Kolehmainen, M., Graham, A. W., et al. 2022, MNRAS, 512, 3284
Spera, M., & Mapelli, M. 2017, MNRAS, 470, 4739
Spinoso, D., Bonoli, S., Valiante, R., Schneider, R., & Izquierdo-Villalba, D. 2023, MNRAS, 518, 4672
Sruthi, K., & Ravikumar, C. D. 2023, MNRAS, 521, 1547
Stone, M. A., Lyu, J., Rieke, G. H., & Alberts, S. 2023a, ApJ, 953, 180
Stone, M. A., Lyu, J., Rieke, G. H., Alberts, S., & Hainline, K. N. 2023b, arXiv e-prints, arXiv:2310.18395
Stone, N. C., Küpper, A. H. W., & Ostriker, J. P. 2017, MNRAS, 467, 4180
Stone, N. C., & Metzger, B. D. 2016, MNRAS, 455, 859
Strader, J., Chomiuk, L., Maccarone, T. J., et al. 2012, ApJL, 750, L27
Strait, V., Brammer, G., Muzzin, A., et al. 2023, ApJL, 949, L23
Strohmayer, T. E., & Mushotzky, R. F. 2009, ApJ, 703, 1386
Strokov, V., Fragione, G., & Berti, E. 2023, MNRAS, 524, 2033
Sun, G., Faucher-Giguère, C.-A., Hayward, C. C., & Shen, X. 2023a, MNRAS, 526, 2665
Sun, W., Ho, L. C., Zhuang, M.-Y., et al. 2023b, arXiv e-prints, arXiv:2308.09076
Tagawa, H., Haiman, Z., & Kocsis, B. 2020, ApJ, 892, 36
Takekawa, S., Oka, T., Iwata, Y., Tsujimoto, S., & Nomura, M. 2019, ApJL, 871, L1
—. 2020, ApJ, 890, 167
Tanikawa, A. 2018, ApJ, 858, 26
Tanikawa, A., Sato, Y., Nomoto, K., et al. 2017, ApJ, 839, 81
The LIGO Scientific Collaboration, the Virgo Collaboration, Abbott, R., et al. 2021, arXiv e-prints, arXiv:2108.01045
Tiley, A. L., Bureau, M., Cortese, L., et al. 2019, MNRAS, 482, 2166
Tody, D. 1986, in Society of Photo-Optical Instrumentation Engineers (SPIE) Conference Series, Vol. 627, Instrumentation in astronomy VI, ed. D. L. Crawford, 733

Tody, D. 1993, in Astronomical Society of the Pacific Conference Series, Vol. 52, Astronomical Data Analysis Software and Systems II, ed. R. J. Hanisch, R. J. V. Brissenden, & J. Barnes, 173
Tolman, R. C. 1930, Proceedings of the National Academy of Science, 16, 511
—. 1934, Relativity, Thermodynamics, and Cosmology (Oxford: Clarendon Press)
Torniamenti, S., Rastello, S., Mapelli, M., et al. 2022, MNRAS, 517, 2953
Torres-Orjuela, A., Huang, S.-J., Liang, Z.-C., et al. 2023, arXiv e-prints, arXiv:2307.16628
Tozzi, G., Maiolino, R., Cresci, G., et al. 2023, MNRAS, 521, 1264
Treiber, H. P., Hinkle, J. T., Fausnaugh, M. M., et al. 2023, MNRAS, 525, 5795
Tremou, E., Strader, J., Chomiuk, L., et al. 2018, ApJ, 862, 16
Treuthardt, P., Seigar, M. S., Sierra, A. D., et al. 2012, MNRAS, 423, 3118
Treuthardt, P. M., Scott, A., & Hewitt, I. B. 2019, in American Astronomical Society Meeting Abstracts, Vol. 234, American Astronomical Society Meeting Abstracts #234, 202.03
Trinca, A., Schneider, R., Maiolino, R., et al. 2023, MNRAS, 519, 4753
Trinca, A., Schneider, R., Valiante, R., et al. 2022, MNRAS, 511, 616
Tripodi, R., Lelli, F., Feruglio, C., et al. 2023, A&A, 671, A44
Tsuboi, M., Kitamura, Y., Tsutsumi, T., et al. 2019, PASJ, 71, 105
—. 2020, PASJ, 72, L5
—. 2017, ApJL, 850, L5
Tully, R. B., & Fisher, J. R. 1977, A&A, 500, 105
Tyson, J. A. 2002, in Society of Photo-Optical Instrumentation Engineers (SPIE) Conference Series, Vol. 4836, Survey and Other Telescope Technologies and Discoveries, ed. J. A. Tyson & S. Wolff, 10–20
Übler, H., Maiolino, R., Curtis-Lake, E., et al. 2023, A&A, 677, A145
Umeda, H., Hosokawa, T., Omukai, K., & Yoshida, N. 2016, ApJL, 830, L34
Umeda, H., Ouchi, M., Nakajima, K., et al. 2022, ApJ, 930, 37
Vajpeyi, A., Smith, R., Thrane, E., et al. 2022, MNRAS, 516, 5309
van den Bergh, S. 1998, Galaxy Morphology and Classification (Cambridge ; New York : Cambridge University Press)
van der Wel, A., Franx, M., van Dokkum, P. G., et al. 2014, ApJ, 788, 28
Van Rossum, G., & Drake, F. L. 2009, Python 3 Reference Manual (Scotts Valley, CA: CreateSpace)
van Wassenhove, S., Volonteri, M., Walker, M. G., & Gair, J. R. 2010, MNRAS, 408, 1139
Vanzella, E., Loiacono, F., Bergamini, P., et al. 2023, A&A, 678, A173
Velazquez, M., & Gezari, S. 2022, in American Astronomical Society Meeting Abstracts, Vol. 54, American Astronomical Society Meeting Abstracts, 243.06
Vergara, M. C., Escala, A., Schleicher, D. R. G., & Reinoso, B. 2023, MNRAS, 522, 4224
Vick, M., Lai, D., & Fuller, J. 2017, MNRAS, 468, 2296
Villforth, C., Herbst, H., Hamann, F., et al. 2019, MNRAS, 483, 2441
Virtanen, P., Gommers, R., Oliphant, T. E., et al. 2020, Nature Methods, 17, 261
Visbal, E., Haiman, Z., & Bryan, G. L. 2014, MNRAS, 445, 1056
Vitral, E., Libralato, M., Kremer, K., et al. 2023, MNRAS, 522, 5740
Volonteri, M., Haardt, F., & Madau, P. 2003, ApJ, 582, 559
Volonteri, M., Habouzit, M., & Colpi, M. 2023, MNRAS, 521, 241
Volonteri, M., Lodato, G., & Natarajan, P. 2008, MNRAS, 383, 1079
Volonteri, M., & Rees, M. J. 2005, ApJ, 633, 624
Wang, L., Tanikawa, A., & Fujii, M. 2022, MNRAS, 515, 5106
Weatherford, N. C., Kıroğlu, F., Fragione, G., et al. 2023, ApJ, 946, 104
Webb, N., Cseh, D., Lenc, E., et al. 2012, Science, 337, 554
Webb, N. A., Barret, D., Godet, O., et al. 2010, ApJL, 712, L107
Webb, N. A., Guérou, A., Ciambur, B., et al. 2017, A&A, 602, A103
Wehner, E. H., & Harris, W. E. 2006, ApJL, 644, L17
Weisskopf, M. C., Tananbaum, H. D., Van Speybroeck, L. P., & O'Dell, S. L. 2000, Society of Photo-Optical Instrumentation Engineers (SPIE) Conference Series, Vol. 4012, Chandra X-ray Observatory (CXO): overview (SPIE), 2–16
Weller, E. J., Pacucci, F., Hernquist, L., & Bose, S. 2022, MNRAS, 511, 2229
Weller, E. J., Pacucci, F., Natarajan, P., & Di Matteo, T. 2023a, MNRAS, 522, 4963
Weller, E. J., Pacucci, F., Ni, Y., et al. 2023b, MNRAS, 520, 3955

Wen, S., Jonker, P. G., Stone, N. C., & Zabludoff, A. I. 2021, ApJ, 918, 46
Weston, M. E., McIntosh, D. H., Brodwin, M., et al. 2017, MNRAS, 464, 3882
Whalen, D. J., Latif, M. A., & Mezcua, M. 2023, ApJ, 956, 133
Whalen, D. J., Mezcua, M., Meiksin, A., Hartwig, T., & Latif, M. A. 2020, ApJL, 896, L45
Will, C. M. 2004, ApJ, 611, 1080
Willett, K. W., Lintott, C. J., Bamford, S. P., et al. 2013, MNRAS, 435, 2835
Williams, D. R. A., Pahari, M., Baldi, R. D., et al. 2022, MNRAS, 510, 4909
Williams, H., Kelly, P. L., Chen, W., et al. 2023a, Science, 380, 416
Williams, J. K., Gliozzi, M., Bockwoldt, K. A., & Shuvo, O. I. 2023b, MNRAS, 521, 2897
Willmer, C. N. A. 2018, ApJS, 236, 47
Willott, C. J., Delorme, P., Omont, A., et al. 2007, AJ, 134, 2435
Wu, X.-B., Wang, F., Fan, X., et al. 2015, Nature, 518, 512
Wu, Y., Cai, Z., Sun, F., et al. 2023, ApJL, 942, L1
Yan, H., Ma, Z., Ling, C., Cheng, C., & Huang, J.-S. 2023, ApJL, 942, L9
Yang, J., Paragi, Z., Frey, S., et al. 2023, MNRAS, 520, 5964
Yang, X., & Yang, J. 2023, Galaxies, 11, 53
Yao, Y., Ravi, V., Gezari, S., et al. 2023, ApJL, 955, L6
Yu, S.-Y., & Ho, L. C. 2018, ApJ, 869, 29
—. 2019, ApJ, 871, 194
—. 2020, ApJ, 900, 150
Yu, S.-Y., Ho, L. C., Barth, A. J., & Li, Z.-Y. 2018, ApJ, 862, 13
Yu, S.-Y., Ho, L. C., & Wang, J. 2021, ApJ, 917, 88
Yuan, W., Zhang, C., Chen, Y., & Ling, Z. 2022, in Handbook of X-ray and Gamma-ray Astrophysics, 86
Zaritsky, D., & Behroozi, P. 2023, MNRAS, 519, 871
Zavala, J. A., Buat, V., Casey, C. M., et al. 2023, ApJL, 943, L9
Zaw, I., Rosenthal, M. J., Katkov, I. Y., et al. 2020, ApJ, 897, 111
Zhang, W. M., Soria, R., Zhang, S. N., Swartz, D. A., & Liu, J. F. 2009, ApJ, 699, 281
Zhu, Z., Li, Z., Ciurlo, A., et al. 2020, ApJ, 897, 135